Title: Tempo and Pattern of Avian Brain Size Evolution

Authors: Daniel T. Ksepka[1,37,38], Amy M. Balanoff[2,37], N. Adam Smith[3,37], Gabriel S. Bever[4], Bhart-Anjan S. Bhullar[5], Estelle Bourdon[6], Edward L. Braun[7], J. Gordon Burleigh[7], Julia A. Clarke[8], Matthew W. Colbert[8], Jeremy R. Corfield[9], Federico J. Degrange[10], Vanesa L. De Pietri[11], Catherine M. Early[12], Daniel J. Field[14], Paul M. Gignac[15], Maria Eugenia Leone Gold[16,17], Rebecca T. Kimball[7], Soichiro Kawabe[18], Louis Lefebvre[19], Jesús Marugán-Lobón[20,21], Carrie S. Mongle[22], Ashley Morhardt[23], Mark A. Norell[24], Ryan C. Ridgely[12], Ryan S. Rothman[22], R. Paul Scofield[11], Claudia P. Tambussi[10], Christopher R. Torres[25], Marcel van Tuinen[26], Stig A. Walsh[27], Akinobu Watanabe[28,29], Lawrence M. Witmer[12], Alexandra K. Wright[30], Lindsay E. Zanno[31,32], Erich D. Jarvis[33,34], and Jeroen B. Smaers[35,36,37]

Affiliations:

[1]Bruce Museum, Greenwich, CT 06830, USA.

[2]Department of Psychological and Brain Sciences, Johns Hopkins University, Baltimore, MD 21218, USA.

[3]Campbell Geology Museum, Clemson University, Clemson, SC 29634, USA.

[4]Center for Functional Anatomy and Evolution, Johns Hopkins University School of Medicine, Baltimore, MD 21205, USA

[5]Department of Geology & Geophysics and Peabody Museum of Natural History, Yale University, New Haven, CT 06511, USA.

[6]Laboratoire Informatique et Systématique, Muséum National d'Histoire Naturelle, 75005 Paris, France.

[7]Department of Biology, University of Florida, Gainesville, FL 32611 USA.

[8]The Jackson School of Geosciences, The University of Texas at Austin, Austin, TX 78712 USA.

[9]Salisbury University, Salisbury, MD 28101, USA.

[10]Centro de Investigaciones en Ciencias de la Tierra, UNC, CONICET, Córdoba, Argentina.

[11]Canterbury Museum, Christchurch 8013, New Zealand.

[12]Department of Biomedical Sciences, Ohio University Heritage College of Osteopathic Medicine, Ohio Center for Ecology and Evolution, Athens, OH 45701, USA.

[14]Department of Earth Sciences, University of Cambridge, Cambridge CB2 3EQ, UK.

[15]Oklahoma State University Center for Health Sciences, Tulsa, OK 74107, USA.

[16]Suffolk University, Boston, MA 02108, USA.

[17]Department of Anatomical Sciences, Stony Brook University, Stony Brook, NY 11794, USA.

[18]Fukui Prefectural Dinosaur Museum, 51-11 Terao, Muroko, Katsuyama, Fukui 911-8601, Japan.

[19]Department of Biology, McGill University, Montréal QC H3A 0G4 Canada.

[20]Departamento de Biología, Universidad Autónoma de Madrid, 28049 Madrid, Spain.

[21]Dinosaur Institute, Natural History Musum of Los Angeles, Los Angeles, CA 90007, USA.

[22]Interdepartmental Doctoral Program in Anthropological Sciences, Stony Brook University, Stony Brook, NY 11794, USA.

[23]Washington University School of Medicine in St. Louis, St. Louis, MO 06130, USA.

[24]Division of Paleontology, American Museum of Natural History, New York, NY 10024, USA.

[25]Department of Integrative Biology, University of Texas at Austin, Austin, TX 78712, USA.

[26]Department of Otorhinolaryngology, University Medical Center, Groningen, the Netherlands.

[27]National Museum of Scotland, Edinburgh EH1 1JF, UK.

[28]Department of Anatomy, New York Institute of Technology, Old Westbury, NY 11568, USA.

[29]Life Sciences Department, Natural History Museum, London SW7 5BD UK.

[30]Vanderbilt University, Nashville, TN 37235, USA.

[31]Paleontology, North Carolina Museum of Natural Sciences, Raleigh, NC 27601, USA.

[32]Department of Biological Sciences, North Carolina State University, Raleigh, NC 27695, USA.

[33]The Rockefeller University, New York, NY 10065, USA.

[34]The Howard Hughes Medical Institute, Chevy Chase, MD 20815, USA.

[35]Department of Anthropology, Stony Brook University, Stony Brook, NY 11794, USA.

[36]Division of Anthropology, American Museum of Natural History, New York, NY 10024, USA.

[37]These authors contributed equally to the work.

[38]Lead contact.

* Correspondence: dksepka@brucemuseum.org

Summary

Relative brain sizes in birds can rival those of primates, but large-scale patterns and drivers of avian brain evolution remain elusive [1-5]. Here, we explore the evolution of the fundamental brain-body scaling relationship [1, 6-8] across the origin and evolution of birds. Using a comprehensive dataset sampling >2,000 modern birds, fossil birds, and non-avian theropod dinosaurs, we infer patterns of brain-body covariation in deep time. Our study confirms that no significant increase in relative brain size accompanied trends towards miniaturization or flight acquisition during the theropod-bird transition [9-12]. Critically, however, theropods and basal birds show weaker integration between brain size and body size, allowing for rapid changes in the brain-body relationship that set the stage for dramatic shifts in early crown birds. We infer that major shifts occurred rapidly in the aftermath of the Cretaceous-Paleogene mass extinction within Neoaves, in which multiple clades achieved higher relative brain sizes due to a reduction in body size. Parrots and corvids achieved the largest brains observed in birds via markedly different patterns: parrots primarily reduced their body size, whereas corvids increased body and brain size simultaneously, with rates of brain size evolution outpacing body size. Collectively, these patterns suggest an early adaptive radiation in brain size that laid the foundation for subsequent selection and stabilization.

RESULTS AND DISCUSSION

Significant deviations from "universal" anatomical scaling relationships provide fundamental insights into common growth laws, and thus help identify major shifts in evolutionary patterns and their causative mechanisms [1-6]. Departures from standard scaling relationships generally align with changes in genetic and developmental regulation [7], and thereby may reveal changes in adaptive profile. Such allometric deviations shape the direction of trait variation on a macroevolutionary scale and consequently underlie much of modern phenotypic diversity [8].

Brain size is one of the most widely studied variables in this framework and has been correlated with major evolutionary innovations such as enhanced sensory capabilities, cognition, social complexity, flight, and environmental adaptability [1-5, 13-15]. Brain size within vertebrates typically scales allometrically, and differences in relative brain size can stem from changes in body size, brain size, or both [1, 15]. Disentangling these variables is key to reconstructing the tempo and pattern of brain evolution. However, a synthetic understanding of brain-body size scaling is not attainable by studying extant taxa alone. Fossils are crucial as non-avian dinosaurs provide a window into changes occurring throughout the phylogenetic trend towards "miniaturization" preceding the evolution of flight [9, 10], and help anchor estimates of ancestral states given the paucity of endocasts available from Mesozoic birds. Moreover, extinct birds, especially flightless taxa (e.g., moa, dodo), may provide insights into encephalization patterns, given that the loss of flight is often accompanied by a rapid increase in body size [16].

Traits such as brain size can be mapped across phylogeny, but properly interpreting trait mapping algorithms can be challenging, especially when the traits of interest share scaling relationships that may themselves be under selection. We implement a suite of methods that collectively allow us to untangle the effects of changes in brain-body size relationships by

considering that both the intercept (mean deviation from the common scaling relationship) and slope (covariation of this relationship) can be under selection [e.g. 17, 18]. Shifts in intercept correspond to differences in mean relative brain size among taxa that share a given slope, whereas shifts in slope correspond to more (or less) rapid changes in brain volume relative to changes in body size [1]. Such changes can be quantified by identifying disparities in the intercept and slope of a phylogenetic regression between different groups. Furthermore, groups that exhibit a high accumulation of residual deviations provide more variation for selection to act upon and can thereby be considered to be more evolutionarily flexible [18].

We assembled a brain endocast dataset sampling 284 extant bird species, 22 extinct bird species, and 12 non-avian theropod dinosaurs, which we combined with a sample of >1900 extant species from the recent study of Sayol et al. [8] (Fig. S1). The inclusion of fossil data has been shown to improve inferences of trait evolution [19, 20], and further allows us to answer questions about patterns of evolution in deep time. Our analyses utilize a two-phase approach. First, we use bivariate multi-regime Ornstein-Uhlenbeck (OU) methods [21-23] to identify where in the phylogeny shifts in slope and intercept occur. Second, we confirm these shifts using generalized least-squares phylogenetic analysis of covariance (pANCOVA) [24, 25] and quantify strength of integration using a Brownian motion rate comparison of allometric residuals among groups [26]. We further identify where in the phylogeny univariate shifts in body size and brain size have occurred by comparing phylogenetic means of brain size and body size among allometric grades [24, 25] in order to estimate whether disproportionate changes in either brain size or body size have influenced allometric shifts in the brain to body size relationship.

Evolution of brain-body allometry in birds

Our OU and pANCOVA analyses identify large-scale allometric differences in the brain size-body size relationship across clades (Fig. 1). The best-fit model identifies four slopes and eleven intercepts, which together comprise eleven grades (Fig. 2, Table 1 and Table S1). This multi grade model shows a significantly better fit relative to a single grade model ($F_{15,2}$=29.56, P<0.001), or to a model that includes only differences in intercepts ($F_{15,12}$=51.08, P<0.001). Mapping these scaling relationships across phylogeny, we identify evolutionary shifts away from the ancestral pattern of brain-body covariation (slope shifts) along nine branches (Fig 1A, asterisks), with nine additional shifts to higher or lower intercepts without a change in slope.

Non-avian dinosaurs and basally diverging birds share a low ancestral slope. Yet, rates of relative brain size evolution are higher along the phylogenetic interval spanning non-avian theropods and the base of the crown bird radiation than for most of the later diverging crown bird groups (Table 2). Among non-avian dinosaurs, there were three independent shifts in grade, all resulting in a higher intercept but no change in slope (Fig. 1A + Fig 3A, shifts from purple grade to grey grade). One of these shifts occurs in Paraves (the clade uniting deinonychosaurian theropods and birds), giving rise to the grade that is retained in *Archaeopteryx* and deeply-diverging crown birds including Palaeognathae ("ratites" and tinamous), Galloanserae (landfowl and waterfowl), Phoenicopterimorphae (grebes and flamingos), and Columbimorphae (pigeons and allies). Three shifts in mean relative brain size occur within clades sharing the ancestral avian grade. Anseriformes (waterfowl) exhibit an increase in intercept, but no significant change in slope (Fig. 2A, teal regression). Apterygiformes (kiwi) show an increase in both intercept and slope, which results in these small, specialized ratites converging with the higher-slope grade characterizing many early-diverging clades of Neoaves (Fig. 2B, green regression). Conversely,

a decrease in intercept, indicating a pronounced decrease in mean relative brain size, is observed within Dinornithiformes (moa) (Fig. 2A, purple regression).

The earliest shift to a higher slope occurs within Neoaves, along the branch uniting all neoavian birds except for the basally-diverging Phoenicopterimorphae and Columbimorphae (Fig. 1A, Fig. 3A). Within Neoaves, a pervasive trend of achieving even higher slopes via continued decrease in body size is observed: this pattern is observed within Apodiformes (in hummingbirds and swifts), Charadriiformes (in sandpipers and buttonquails), and five times within Telluraves (see below). Aequornithia (waterbirds) contradict this general pattern and are unique in showing a pattern in which both body size and brain size increase in almost the same proportion. This nevertheless results in a higher slope because brain size is expected to increase at ~0.6 body size increase due to scaling relationships [1].

Interestingly, the branch leading to Telluraves ("higher landbirds") is characterized by a marked decrease in slope, which corresponds to a major increase in body size (Fig. 1A, Fig. 3A). Both sides of the basal divergence in Telluraves are occupied by pairs of successively branching predatory clades [27] (Fig. 1A, clades in red font), which share a low slope while maintaining a high intercept: Accipitriformes (hawks, vultures, and allies) and Strigiformes (owls) on the Afroaves side, and Falconiformes (falcons), and Cariamiformes (seriemas and the extinct "terror birds") on the Australaves side. Owls notably retain the ancestral Telluraves slope but shift to a higher intercept. Subsequently, multiple nested shifts to higher grades occur within Afroaves and Australaves: Coraciimorphae (mousebirds, rollers, and allies) shift to a higher slope and Picidae (woodpeckers) to a higher intercept in Afroaves, whereas Psittacopasserae (passerines and parrots) shift to a higher slope. Psittaciformes, Ptilonorhynchidae (bowerbirds) and Corvidae shift to a higher intercept in Australaves.

Two caveats should be recognized. First, the shift towards a higher intercept in bowerbirds coincides with a downward shift in slope, but due to low sample size (n=10) there is not enough information to statistically establish whether bowerbirds align more with owls (AIC weight 0.526) or with parrots, corvids and woodpeckers (AIC weight 0.473). Because bowerbirds are nested well within Passeriformes, we consider it more parsimonious to assume that they share the ancestral passerine slope and are thus aligned with parrots, corvids and woodpeckers (as depicted in Figures 1 and 2) but with the recognition that future work is needed to test this scenario. Second, while a single-slope regression is extremely useful for a heuristic visual comparison of relative brain size across all taxa (Figure 1B), this can result in underestimation/overestimation for specific taxa. For example, the single slope regression is an underestimation of the high slope shared by Coraciimorphae, so relative brain size will be overestimated in large-bodied taxa in that clade (e.g. hornbills). Thus Figures 2 and 3A provide the most accurate overall representation of our results.

Our results are robust to sampling and modeling assumptions: we recover the same major patterns when constraining the tree to accommodate a shift along the avian stem lineage, comparing "early" versus "late" radiating clades, and excluding fossil taxa (Fig. S2-S4, Tables S2).

Shifts in brain-body integration during the Paleogene crown bird radiation

The strength of brain-body integration can be approximated by examining the rate of evolution of residual allometric deviations, with higher rates indicating increased decoupling of the brain-body relationship. In our analysis, concomitant with shifts in brain-body allometry immediately following the K-Pg mass extinction, we observe a significant shift in brain-body

integration. Intriguingly, this shift is towards lower rather than higher rates of evolution and thus implies a stronger degree of integration. Rates of brain-body size evolution are high in theropods and early-diverging crown birds (Palaeognathae, Galloanserae, Phoenicopteriformes, and Columbimorphae) and shift to significantly lower rates early in the Paleogene radiation of Neoaves (Table 2). Although a decrease in body size is an important factor in this rate decrease, this finding is not an artifact of including large-bodied non-avian dinosaurs: a significantly higher rate of evolution is observed among early diverging crown birds (Palaeognathae and Galloanserae) versus Neoaves in supplementary analyses including only extant taxa (rate ratio of 1.56, $P<0.001$).

In contrast to the lower rates that characterize most neoavians, a shift towards the highest rate of relative brain size evolution identified across all birds takes place in corvids, accompanying the shift to a higher slope in this clade (Table 2). A marked decrease in the strength of brain-body integration may thus have facilitated selection for increased brain size in these birds. Significant but less dramatic rate shifts are observed in parrots, owls, and waterfowl (Table 2).

Diverse patterns of brain-body size changes underpin allometric shifts

Our findings reveal that numerous combinations of brain and body size evolution drove changes in relative brain size within major clades of birds. The initial shift to a higher grade in the expansive neoavian radiation appears to have been driven by rates of body size decrease greatly outpacing rates of brain volume decrease, resulting in larger average brain volumes at a given body mass (Table 3). Subsequently, at the base of the telluravian landbird radiation, the opposite pattern is observed with a marked increase in body size outpacing a simultaneous

increase in brain size. This coincides with a shift to a carnivorous diet that characterizes four basally diverging telluravian clades (Accipitriformes, Strigiformes, Falconiformes, and Cariamiformes). Despite having relatively large brains in comparison to other neoavians, all four predatory clades share the low slope ancestral for birds, indicating a lower rate of brain evolution relative to body size evolution. This pattern is particularly striking as it parallels well-characterized patterns in mammalian carnivorans, in which changes in relative brain size have been attributed largely to body size evolution rather than selection for neuronal capacity [15]. Our data suggest that strong body size selection in raptorial birds linked to their preferred prey classes (e.g. small rodents versus large waterfowl) may have been the most important driver of the brain-body relationship in early Telluraves.

Intriguingly, parallel shifts toward higher slopes accompany independent transitions away from predatory ecologies in the two major clades of Telluraves. In Afroaves, Coraciimorphae show a secondary decrease in body size that leads them to exhibit a higher slope, and in Australaves this pattern is mirrored by a secondary decrease in body size accompanying a shift to a higher slope in Psittacopasserae. Further decreases in body size leading to higher-intercept grades occur within Picidae (in Afroaves) and Psittaciformes (in Australaves). Afroaves and Australaves are not complete parallels, however, as parrots achieve much larger relative brain sizes than do woodpeckers, and the second largest-brained bird (Corvidae) clade also evolves within Australaves via a unique pathway. Corvidae (crows and allies) achieve a higher-intercept grade by simultaneous increases in body size and brain size, with the latter greatly outstripping the former. Parrots and corvids are unique not only for their large brains but also for exhibiting the highest inferred rates of brain-body evolution within Neoaves (Table 2).

Not all shifts, however, led to larger relative brain sizes. In some species of moa (Dinornithidae) relative brain size dropped to a level comparable with that of non-avian theropods because body size increased dramatically with less concomitant change in brain volume (Table 3). Such dichotomies in patterns of brain and/or body size change underpin allometric shifts across the avian tree of life, emphasizing that changes in encephalization are not unequivocally related to selection on brain size alone [15].

Inferring patterns and drivers of avian brain evolution

We infer that a general trend towards larger relative brain size along the backbone of the crown bird tree (Fig 1B, Fig. 3B) was initially driven primarily by selection for smaller body size. However, selection for brain size appears to take over as the primary driver in the largest-brained birds. Counterintuitively, rates of evolution are higher along the phylogenetic interval spanning non-avian theropods and the base of the crown bird radiation and slow down within Neoaves (Table 2). This observation may be due in part to body size not being constrained by the aerodynamic demands of flight in non-avian dinosaurs; however, this pattern remains when fossil taxa are excluded. An early interval during which a high rate of evolution prevailed may have set the stage for selection to act on a wider range of encephalization levels in early crown birds. Rates of evolution appear to have stabilized over time, while directional selection acted on individual clades. This interval was punctuated by the more recent, pronounced rate increases in corvids, parrots, and owls.

Our inference of a shared scaling relationship between crownward non-avian theropods, *Archaeopteryx*, and basally diverging crown birds (i.e. most palaeognaths, landfowl, and basal neoavians) is in concordance with findings from previous studies. Such studies have found that,

despite a trend towards body size reduction and the acquisition of flight having occurred along the avian stem lineage, there is no evidence for major shifts in relative brain size associated with the divergence of *Archaeopteryx* (i.e., near the origin of powered flight) nor the origin of crown birds [11, 12]. While this does not preclude morphological changes in regional brain shape (which is often plastic even within modern bird families), previous studies have concluded that no significant changes in the relative volume of the cerebrum or cerebellum occurred along the transition from Paraves to basal crown birds [12].

It is compelling to note that only three grade shifts are inferred across the phylogenetic interval spanning Paraves to Neoaves, and only one of these (that in Anseriformes) is inferred to have taken place in the Cretaceous. In contrast, fifteen grade shifts, including nine resulting in new slopes, are inferred during the Paleocene (Fig. 3A). Thus, we infer that the most profound shifts in both brain-body size covariation and relative brain size occurred not at the origin of flight or the appearance of crown birds, but rather during the major ecological radiation of Neoaves following the K-Pg mass extinction [30-32]. This pattern aligns with the principles of adaptive radiation, in which early diversification is followed by directional changes in adaptive profile and slowdowns in rates of evolution [33]. The impact on present day diversity is evident in the larger range of overall relative brain sizes exhibited by Neoaves versus the more restricted range in basally diverging birds (Fig. 4).

Our results demonstrate that despite the divergence between non-avian theropods and Avialae occurring >150 million years ago, birds only reached their apex in relative brain size recently, with crown corvids and crown parrots estimated to have radiated in the Neogene [28] (Fig. 4). The finding that these taxa share both the highest inferred rates of brain-to-body evolution among Neoaves and the steepest allometric slopes among all birds raises the question

of what common factors may underlie their shared trajectories. Parrots, oscine songbirds (including corvids), and hummingbirds (Trochilidae) are the only major bird groups known to be capable of vocal learning, an ability controlled by additional brain pathways not found in other birds [34]. This complex behavior and associated neuroanatomical features represent a plausible driver of increased brain size in parrots. The case is more complex within oscine songbirds and hummingbirds. Most oscines share the same ancestral slope as suboscines, all but a few of which lack vocal learning. Hummingbirds likewise share the same ancestral slope as the non-vocal learning swifts. Although hummingbirds have exceptionally large brains as a raw proportion of body size, this appears to be almost exclusively an effect of negative allometry (i.e. smaller birds are expected to have proportionally larger brains). Thus, hummingbirds fall comfortably within the range of relative brain sizes observed in other early-diverging clades of Neoaves.

Recent studies suggest that high levels of encephalization may be due to differential growth of individual brain regions as opposed to their concerted evolution [12, 35-37]. This hypothesis is supported by the observation that proportions of major neuroanatomical divisions vary widely in size among different groups of large-brained birds [35, 38-40]. Parrots and oscine songbirds are similar to mammals in that their high encephalization values are primarily the product of increasing the relative size of the cerebral cortical regions [36]. In contrast, waterbirds exhibit an increase in the relative size of the cerebellum [12] and owls show expanded vestibular and somatosensory nuclei [41].

Corvids provide an intriguing example of convergent brain evolution between birds and hominins, as these groups share a pattern in which brain volume and body size expanded simultaneously, with the former outpacing the latter [15]. Parrots also show convergence with large-brained primates, but in a different way. Parrots, like humans, have recently been shown to

have an additional vocal learning pathway not found in songbirds [45] and a disproportionately expanded telencephalic-midbrain-cerebellar circuit, thus showing not only volumetric but also structural convergence with hominoids [44, 45].

Corvids and parrots exhibit impressive relative brain sizes, but basic volumetric indices likely underestimate their true neurological complexity. These groups exhibit the highest-known cerebral neuronal densities in birds, and raw neuronal counts in individual parrots and crows rival those of some primates despite a smaller absolute brain size [44]. This increased neuron density has been suggested to accommodate enhanced brain pathways, such as those for vocal learning [44]. Thus, the increase in cognitive complexity in parrots and corvids versus other birds may be a result of concomitant increases in not only relative brain volume but also neuron density, facilitating additional brain pathways.

Our data reveal the complex and dynamic evolutionary history of avian encephalization. This history includes high early rates of evolution that stabilized across the theropod-bird transition, a subsequent series of profound grade shifts as crown birds adapted to myriad ecologies early in the Cenozoic, and a culmination in which two groups—parrots and corvids—independently acquired relative brain sizes, neuron densities, and sophisticated cognitive potential near the pinnacle of the vertebrate world.

ACKNOWLEDGMENTS

We thank Ruger Porter and Loic Costeur for processing additional endocasts, and Josef C. Uyeda for advice using the bayou R package. This project was supported by the NESCent (NSF EF-0905606) Catalysis Meeting grant “A Deeper Look into the Avian Brian: Using Modern Imaging to Unlock Ancient Endocasts” Additional support was derived from awards NSF DEB 1457181

to A.M.B., G.S.B., P.M.G., and M.A.N., NSF DEB 1655736 to D.T.K., NSF DEB 1655683 to E.L.B. and R.L.K., NSF DEB 0949897 to JAC, PIP 0437 and 0059 to C.P.T. and F.J.D., HHMI support to E.D.J., CGL2013-42643-P to J.M.-L., NERC NE/H012176/1 to S.A.W., and Marsden grant CTM1601 to V.L.D.P. and R.P.S.

AUTHOR CONTRIBUTIONS

D.T.K., A.M.B, and N.A.S. organized the NESCent project that initiated this research. All authors except E.B., E.L.B., G.S.B., V.L.D., R.K., S.K. participated in the planning of the project at the NESCent Catalysis Meeting. D.T.K., A.M.B., N.A.S., G.S.B., J.A.C., F.J.D., V.L.D., C.M.E, M.E.L.G., S.K., J.M.-L., A.C.M., M.A.N., R.C.R., R.P.S., C.P.T., M.V., L.M.W., S.A.W., A.K.W., and L.E.Z. contributed endocast data. J.G.B., E.L.B., R.L.K., and D.T.K. generated the dated phylogenies. J.B.S. completed the comparative analyses with assistance from R.S.R. and C.S.M.. D.T.K, A.M.B., N.A.S., J.B.S., and E.D.J. drafted the manuscript and all authors contributed to editing the paper.

DECLARATION OF INTERESTS

The authors declare no competing interests.

REFERENCES

1. Jerison, H. (1973). Evolution of the Brain and Intelligence (Academic Press).
2. Madden, J. (2001). Sex, bowers and brains. Proc. Roy. Soc. B *268*, 833-838.
3. Lefebvre, L., Nicolakakis, N., and Boire, D. (2002). Tools and brains in birds. Behaviour *139*, 939–973.
4. Cnotka, J., Güntürkün, O., Rehkämper, G., Gray, R. D., and Hunt, G.R. (2008). Extraordinary

large brains in tool-using New Caledonian crows (*Corvus moneduloides*). Neuroscience Letters *433*, 241-245.

5. Overington, S. E., Morand-Ferron, J., Boogert, N.J., Lefebvre, L. (2008). Technical innovations drive the relationship between innovativeness and residual brain size in birds. Anim. Behav. *78*, 1001–1010.

6. Thompson, D. W. (1917). On Growth and Form (Cambridge University Press).

7. Pélabon C*, et al.* (2014). Evolution of morphological allometry. *Annals of the New York Academy of Sciences* 1320, 58-75.

8. Voje, K.L., Hansen, T.F., Egset, C.K., Bolstad, G.H., and Pelabon, C. (2014). Allometric constraints and the evolution of allometry. Evolution *68*, 866-885.

9. Turner, A.H., Pol, D., Clarke, J.A., Erickson, G.M., and Norell, M.A. (2007). A basal dromaeosaurid and size evolution preceding avian flight. Science *317*(5843), 1378-1381.

10. Lee, M.S.Y., Cau, A., Naish, D., and Dyke, G.J. (2014). Sustained miniaturization and anatomical innovation in the dinosaurian ancestors of birds. Science *345*, 562-566.

11. Balanoff, A.M., Bever, G.S., Rowe, T.B., and Norell, M.A. (2013). Evolutionary origins of the avian brain. Nature *501*, 93-96.

12. Balanoff, A.M., Smaers, J.B., and Turner, A.H. (2016). Brain modularity across the theropod-bird transition: testing the influence of flight on neuroanatomical variation. Journal of Anatomy *229*, 204–214.

13. Schuck-Paim, C., Alonso, W.J., Ottoni, E.B. (2008). Cognition in an ever-changing world: climatic variability is associated with brain size in Neotropical parrots. Brain Behav. Evolut *71*, 200-215.

14. Sayol, F., Maspons, J., Lapiedra, O., Iwaniuk, A.N., Székely, T., Sol, D. (2018). Environmental

variation and the evolution of large brains in birds. Nat. Commun. *7*, 13971.

15. Smaers, J.B., Dechmann, D.K., Goswami, A., Soligo, C., and Safi, K. (2012). Comparative analyses of evolutionary rates reveal different pathways to encephalization in bats, carnivorans, and primates. Proceedings of the National Academy of Sciences *109*, 18006-18011.

16. McMahon, T.A., Bonner, J.T. (1983). On Size and Life. (Scientific American Library).

17. Stillwell, R.C., Shingleton, A.W., Dworkin, I., and Frankino, W.A. (2016). Tipping the scales: evolution of the allometric slope independent of average trait size. Evolution *70*, 433-444.

18. Smaers, J.B., Mongle, C.S., Safi, K., and Dechmann, D.K.N. (2019). Allometry, evolution and development of neocortex size in mammals. Progress in Brain Research *250,* 83-107.

19. Slater, G.J., Harmon, L.J., and Alfaro, M.E. (2012). Integrating fossils with molecular phylogenies improves inference of trait evolution. Evolution *66*, 3931-3944.

20. Finarelli, J.A., Flynn, J.J. (2006). Ancestral state reconstruction of body size in the Caniformia (Carnivora, Mammalia): the effects of incorporating data from the fossil record. Systematic Biology *55*, 301-313.

21. Ingram, T. and Mahler, D.L. (2013). SURFACE: detecting convergent evolution from comparative data by fitting Ornstein-Uhlenbeck models with stepwise Akaike Information Criterion. Methods in Ecology and Evolution *4*, 416-425.

22. Khabbazian, M., Kriebel, R., Rohe, K., and Ané, C. (2016). Fast and accurate detection of evolutionary shifts in Ornstein–Uhlenbeck models. Methods in Ecology and Evolution *7*, 811-824.

23. Uyeda, J.C. and Harmon, L.J. (2014). A novel Bayesian method for inferring and interpreting the dynamics of adaptive landscapes from phylogenetic comparative data. Systematic Biology *63*, 902-918.

24. Smaers, J.B. and Rohlf, F.J. (2016). Testing species' deviation from allometric predictions using the phylogenetic regression. Evolution *70*, 1145-1149.

25. Smaers, J.B., Mongle, C.S. (2018). evomap: R package for the evolutionary mapping of continuous traits: Github: https://github.com/JeroenSmaers/evomap dfa7dfd.

26. Adams, D.C. (2014). Quantifying and comparing phylogenetic evolutionary rates for shape and other high-dimensional phenotypic data. Syst. Biol. *63*, 166-177.

27. Jarvis, E.D. et al. (2014). Whole-genome analyses resolve early branches in the tree of life of modern birds. Science *346*, 1320-1331.

28. Prum, R.O. et al. (2015). A comprehensive phylogeny of birds (Aves). using targeted next-generation DNA sequencing. Nature *526*, 569-573.

29. Reddy, S. et al. (2017). Why do phylogenomic data sets yield conflicting trees? Data type influences the avian tree of life more than taxon sampling. Syst. Biol. *66*, 857-879.

30. Feduccia, A. (1995). Explosive evolution in tertiary birds and mammals. Science *267*, 637–638.

31. Mayr, G. (2009). Paleogene Fossil Birds (Springer).

32. Field, D.J., et al. (2018). Early evolution of modern birds structured by global forest collapse at the end-cretaceous mass extinction. Current Biology *28,* 1-7.

33. Gavrilets, S., Losos, J.B. (2009). Adaptive radiation: contrasting theory with data. Science *323*, 732-737.

34. Petkov, C.I., Jarvis, E. (2012). Birds, primates, and spoken language origins: behavioral phenotypes and neurobiological substrates. Front. Evolut. Neurosci. *4*, 12.1-12.24.

35. Iwaniuk, A.N., Dean, K.M., and Nelson, J.E. (2004). A mosaic pattern characterizes the evolution of the avian brain. Proc. Roy. Soc. Lond. B *271*, S148–S151.

36. Iwaniuk, A.N., Dean, K.M., and Nelson, J.E. (2005). Interspecific allometry of the brain and

brain regions in parrots (Psittaciformes): comparisons with other birds and primates. Brain, Behavior and Evolution *65*, 40–59.

37. Smaers, J.B., Gómez-Robles, A., Parks, A.N., Sherwood, C.C. (2017), Exceptional evolutionary expansion of the prefrontal cortex in great apes and humans. Curr. Biol. *27*, 714-720.

38. Kawabe, S., Shimokawa, T., Miki, H., Matsuda, S., and Endo, H. (2013). Variation in avian brain shape: relationship with size and orbital shape. Journal of Anatomy *223*, 495-508.

39. Marugán-Lobón, J., Watanabe, A., Kawabe, S. (2016). Studying avian encephalization with geometric morphometrics. J. Anat. *229*, 191-203.

40. Balanoff, A.M., Bever, G.S. (2017).The role of endocasts in the study of brain evolution. Evolution of Nervous Systems, Vol. 1, ed Kaas J. (Elsevier), pp 223–241.

41. Sultan, F. (2005). Why some bird brains are larger than others. Curr. Biol. 15, R649-R650.

42. Walsh, S.A., Milner, A.C., Bourdon, E. (2016). A reappraisal of Cerebavis cenomanica (Aves, Ornithurae), from Melovatka, Russia. J. Anat. *229*, 215-227.

43. Field, D.J., Hanson, M., Burnham, D., Wilson, L.E., Super, K., Ehret, D., Ebersole, J.A., Bhullar, B.A.S. (2018). Complete Ichthyornis skull illuminates mosaic assembly of the avian head. Nature *557*, 96-100.

44. Olkowicza, S., et al. (2015). Birds have primate-like numbers of neurons in the forebrain. Proceedings of the National Academy of Sciences, *113*, 7255–7260.

45. Chakraborty, M. et al. (2015). Core and shell song systems unique to the parrot brain (2015). PLoS One *10*, e0118496.

47. Iwaniuk, A., Nelson, J. (2002). Can Endocranial volume be used as an estimate of brain size in birds? Canadian Journal of Zoology *80*, 16-23.

48. Balanoff, A.M., et al. (2016). Best practices for digitally constructing endocranial casts:

examples from birds and their dinosaurian relatives. J Anat *229*, 173-190.

49. Dunning Jr., J.B. (2008). CRC Handbook of Avian Body Masses, 2nd Edition (CRC Press).

50. Field, D.J., Lynner, C., Brown, C., and Darroch, S.A.F. (2013). Skeletal correlates for body mass estimation in modern and fossil flying birds. Plos One *8*, e82000.

51. Christiansen, P. and Farina, R.A. (2004). Mass prediction in theropod dinosaurs. Historical Biology *16*, 85-92.

52. Burleigh, J.G., Kimball, R.T., Braun, E.L. (2015). Building the avian tree of life using a large-scale sparse supermatrix. Molecular Phylogenetics and Evolution *84*, 53-63.

53. Stamatakis, A. (2014). RAxML version 8: a tool for phylogenetic analysis and post-analysis of large phylogenies. Bioinformatics *30*, 1312-1313.

54. Sanderson, M.J. (2002). Estimating absolute rates of molecular evolution and divergence times: a penalized likelihood approach. Molecular Biology and Evolution *19*, 101.

55. Sanderson, M.J. (2003). r8s: Inferring absolute rates of molecular evolution and divergence times in the absence of a molecular clock. Bioinformatics *19*, 301-302.

56. Turner, A.H., Makovicky, P.J., and Norell, M.A. (2012). A review of dromaeosaurid systematics and paravian phylogeny. Bulletin of the American Museum of Natural History *371*, 1-206.

57. Maddison, W.P., and Maddison, D.R. (2015). Mesquite: A modular system for evolutionary analysis. Version 3.04.

58. Uyeda, J.F., Eastman, J., Harmon, L. (2014). bayou: Bayesian fitting of Ornstein-Uhlenbeck models to phylogenies: R package version 1.0.1. http://CRAN.R-project.org/package=bayou.

59. Hansen, T.F. (1997). Stabilizing selection and the comparative analysis of adaptation. Evolution *51*, 1341-1351.

60. Uyeda, J.C., Pennell, M.W., Miller, E.T., Maia, R., and McClain, C.R. (2017). The evolution of

energetic scaling across the vertebrate Tree of Life. The American Naturalist *190*, 185-199.

61. Ho, L. S. T., and Ané, C. (2014). Intrinsic inference difficulties for trait evolution with Ornstein-Uhlenbeck models. Methods in Ecology and Evolution, *5*, 1133-1146.

62. Smaers, J.B., Mongle, C.S., and Kandler, A. (2016). A multiple variance Brownian motion framework for the estimation of ancestral states and rates of evolution. Biol. J. Linn. Soc. *118*, 78-94.

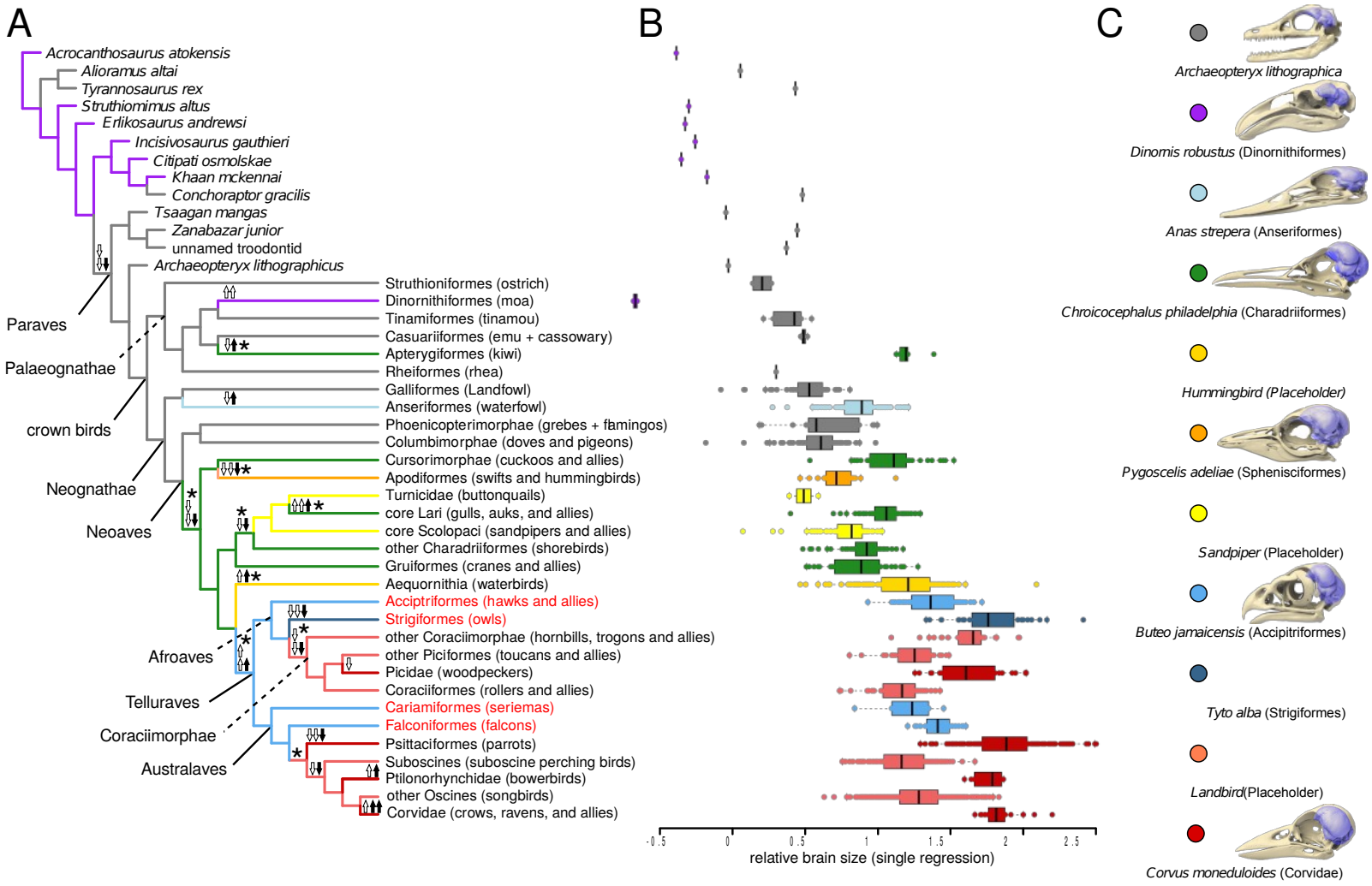
A
Acrocanthosaurus atokensis
Alioramus altai
Tyrannosaurus rex
Struthiomimus altus
Erlikosaurus andrewsi
Incisivosaurus gauthieri
Citipati osmolskae
Khaan mckennai
Conchoraptor gracilis
Tsaagan mangas
Zanabazar junior
unnamed troodontid
Archaeopteryx lithographicus
Paraves
Palaeognathae
crown birds
Neognathae
Neoaves
Afroaves
Telluraves
Coraciimorphae
Australaves
Struthioniformes (ostrich)
Dinornithiformes (moa)
Tinamiformes (tinamou)
Casuariiformes (emu + cassowary)
Apterygiformes (kiwi)
Rheiformes (rhea)
Galliformes (Landfowl)
Anseriformes (waterfowl)
Phoenicopterimorphae (grebes + flamingos)
Columbimorphae (doves and pigeons)
Cursorimorphae (cuckoos and allies)
Apodiformes (swifts and hummingbirds)
Turnicidae (buttonquails)
core Lari (gulls, auks, and allies)
core Scolopaci (sandpipers and allies)
other Charadriiformes (shorebirds)
Gruiformes (cranes and allies)
Aequornithia (waterbirds)
Acciptriformes (hawks and allies)
Strigiformes (owls)
other Coraciimorphae (hornbills, trogons and allies)
other Piciformes (toucans and allies)
Picidae (woodpeckers)
Coraciiformes (rollers and allies)
Cariamiformes (seriemas)
Falconiformes (falcons)
Psittaciformes (parrots)
Suboscines (suboscine perching birds)
Ptilonorhynchidae (bowerbirds)
other Oscines (songbirds)
Corvidae (crows, ravens, and allies)
B
-0.5
0
0.5
1
1.5
2
2.5
relative brain size (single regression)
C
Archaeopteryx lithographica
Dinornis robustus (Dinornithiformes)
Anas strepera (Anseriformes)
Chroicocephalus philadelphia (Charadriiformes)
Hummingbird (Placeholder)
Pygoscelis adeliae (Sphenisciformes)
Sandpiper (Placeholder)
Buteo jamaicensis (Accipitriformes)
Tyto alba (Strigiformes)
Landbird(Placeholder)
Corvus moneduloides (Corvidae)

Figure 1. Avian Brain-Body Size Evolution

(A) Simplified phylogeny of non-avian theropods and birds using phylogenetic backbone from [27]. Branch colors correspond to the eleven significantly different adaptive grades ($F_{15,2}$=29.56, P<0.001, AICΔ=343.53, AICω>0.99) identified in this study. Positions of inferred grade shifts in body size (white arrows) and brain volume (black arrows) are indicated. Double arrows indicate one of these variables changing faster than the other after considering the allometric relationship between the two. Asterisks indicate shifts in slope. Predatory bird clades are indicated in red font. (B) Brain size residuals standardized to a "one slope - one intercept" allometry, to provide a simplified visualization of relative brain size. (C) Skulls and endocasts of representative taxa from each of the eleven grades identified.

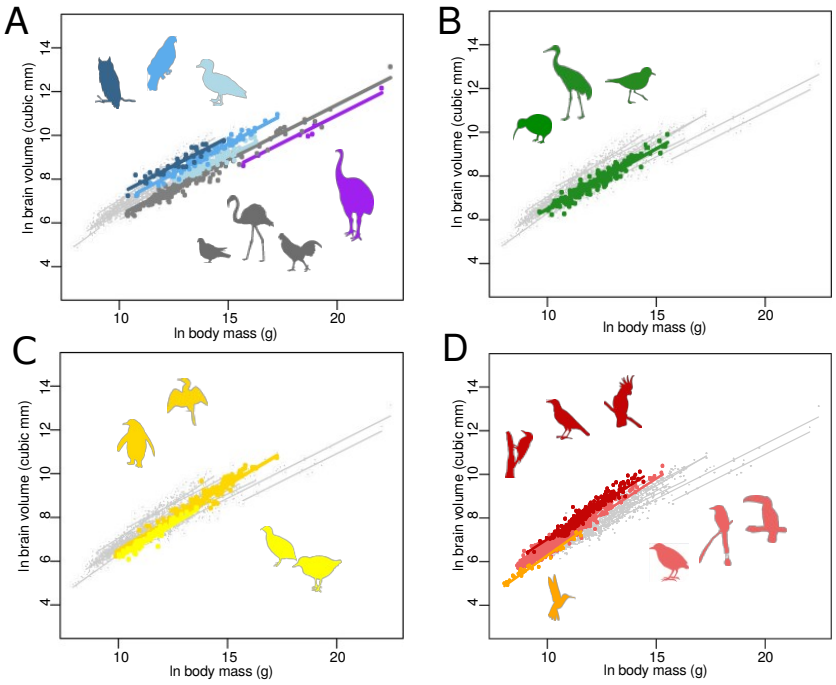

480

481 **Figure 2. Adaptive Grades of Relative Brain Size**

482 (A) Regressions for the five low-slope adaptive grades characterizing non-avian theropods,
483 early-diverging birds (Palaeognathae, basal Neognathae), waterfowl (Anseriformes), and
484 predatory telluravians. (B) Regression for the intermediate-slope grade characterizing most
485 neoavians and kiwi. (C) Regressions for the two high-slope grades characterizing waterbirds
486 (Aequornithes) and some shorebirds (Charadriiformes). (D) Regressions for the three highest-
487 slope grades characterizing Apodiformes, Coraciimorphae, woodpeckers, passerines, and parrots.
488 Colors correspond to those used in Figure 1.

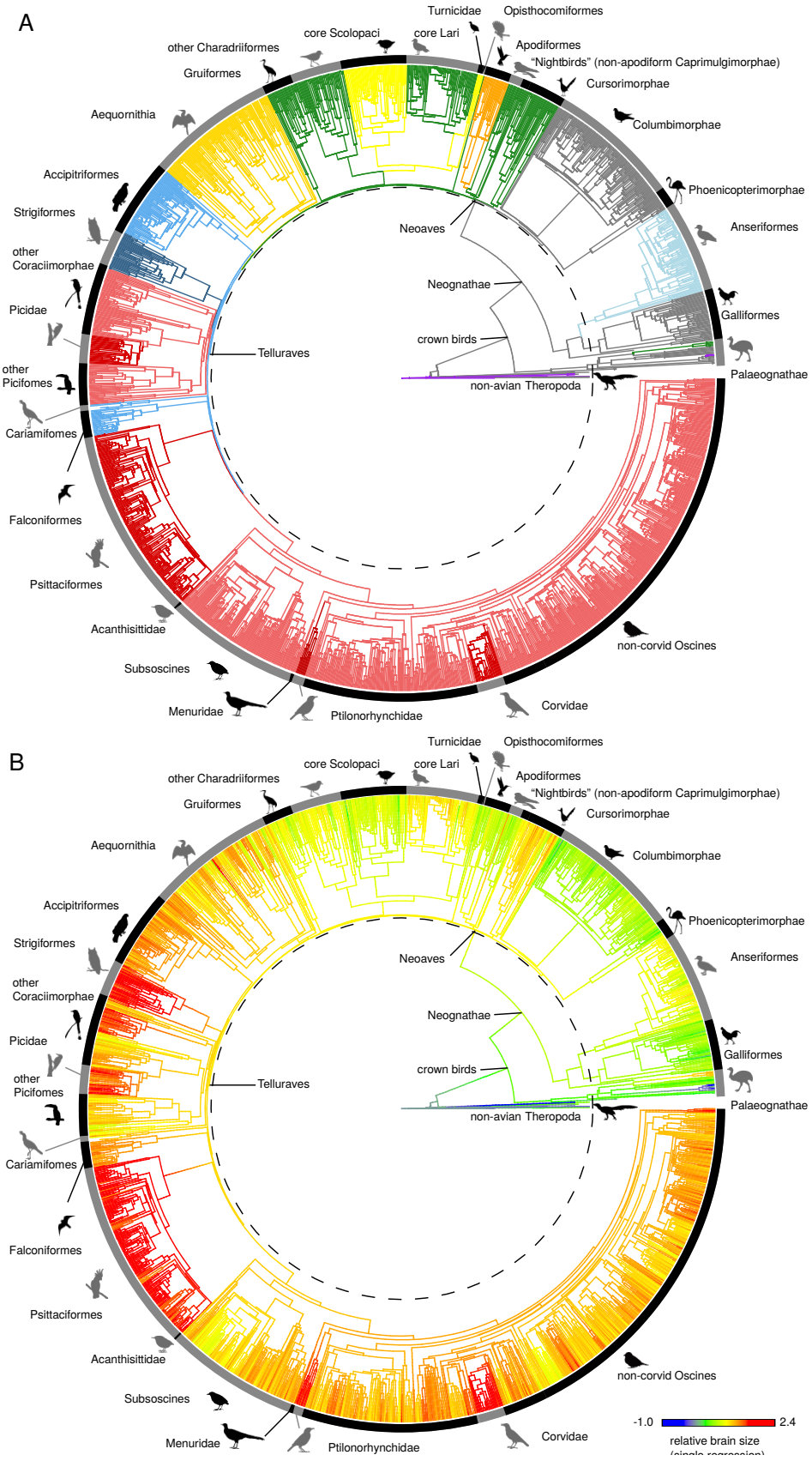
A
Turnicidae
Opisthocomiformes
core Scolopaci
core Lari
other Charadriiformes
Apodiformes
Gruiformes
"Nightbirds" (non-apodiform Caprimulgimorphae)
Cursorimorphae
Aequornithia
Columbimorphae
Accipitriformes
Phoenicopterimorphae
Strigiformes
Neoaves
Anseriformes
other Coraciimorphae
Neognathae
Picidae
Galliformes
crown birds
Telluraves
Palaeognathae
other Picifomes
non-avian Theropoda
Cariamifomes
Falconiformes
Psittaciformes
Acanthisittidae
non-corvid Oscines
Subsoscines
Menuridae
Ptilonorhynchidae
Corvidae
B
Turnicidae
Opisthocomiformes
core Scolopaci
core Lari
other Charadriiformes
Apodiformes
Gruiformes
"Nightbirds" (non-apodiform Caprimulgimorphae)
Cursorimorphae
Aequornithia
Columbimorphae
Accipitriformes
Phoenicopterimorphae
Strigiformes
Neoaves
Anseriformes
other Coraciimorphae
Neognathae
Picidae
Galliformes
crown birds
Telluraves
Palaeognathae
other Picifomes
non-avian Theropoda
Cariamifomes
Falconiformes
Psittaciformes
Acanthisittidae
non-corvid Oscines
Subsoscines
Menuridae
Ptilonorhynchidae
Corvidae
-1.0
2.4
relative brain size

Figure 3. Patterns and Rates of Relative Brain Size Evolution

(A) Time-calibrated phylogeny of theropods and birds included in the endocast dataset illustrating the eleven brain-body size grades identified in this study. (B) Ancestral state estimation [62] of brain size residuals standardized to a "one slope - one intercept" allometry. Colors in (A) correspond to the adaptive grades illustrated in Figure 1. Dashed line in (A) and (B) indicates the K-Pg boundary.

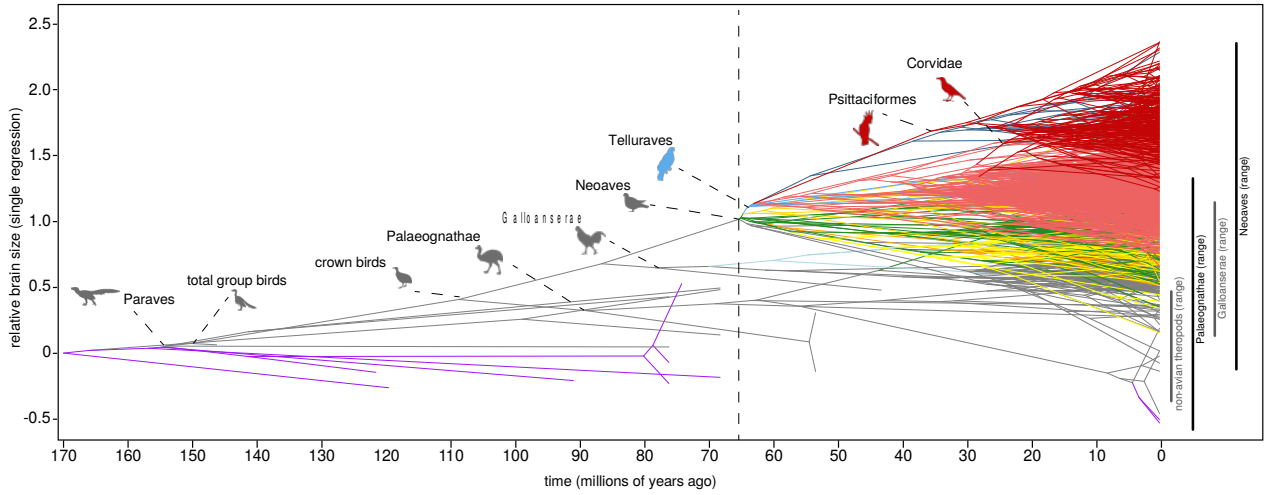

496

497 **Figure 4. Evolution of Variation in Relative Brain Size**

498 Phenogram showing relative brain size over time in non-avian theropods and birds. Colors correspond to the adaptive grades

499 illustrated in Figure 1. Dashed line indicates the K-Pg boundary.

500

Grade	Slope	Slope SE	Intercept	Intercept SE
Non-avian theropods (purple)	0.499	0.017	0.92	0.344
Paraves including early birds (grey)	0.504	0.010	1.309	0.216
Anseriformes: waterfowl (teal)	0.473	0.024	1.972	0.362
“Intermediate” Neoaves (green)	0.555	0.016	0.925	0.214
Apodiformes: swifts & hummingbirds (orange)	0.716	0.024	-0.862	0.250
Charadriiformes (part): sandpipers & buttonquail (yellow)	0.613	0.001	0.002	0.091
Aequornithia: waterbirds (gold)	0.595	0.019	0.544	0.275
Birds of prey: hawks, falcons, seiramas (light blue)	0.521	0.018	1.785	0.281
Strigiformes: owls (dark blue)	0.516	0.031	2.159	0.396
Coraciimorphae: rollers & allies (pink)	0.640	0.015	0.145	0.175
Piciformes: woodpeckers (red, part)	0.700	0.045	-0.097	0.488
Psittaciformes: parrots (red, part)	0.635	0.017	0.795	0.236
Passeriformes: passerines (pink, part)	0.647	0.007	0.201	0.111
Ptilonorhynchidae: bowerbirds (red, part)	0.547	0.067	1.743	1.035
Corvidae: crows and ravens (red, part)	0.660	0.018	0.435	0.241

Table 1. Regression parameters of all grades identified in the primary analysis, derived from pGLS (with lambda transformation) analyses. Colors refer to those depicted in Figure 2. The individual clades that contribute to the highest slope grades are broken out separately for illustrative purposes.

σ^2		Corvi.	Thero.	Psitt.	Strig.	Charl	Anser.	Para.	BoP	Pic.	Aequ.	Ptil.	Neo.	Cora.	Pass.	Apod.
0.0157	Corvidae	**18.64**	**5.88**	**4.81**	**4.07**	**4.03**	**3.61**	**2.55**	**2.44**	**2.31**	**1.97**	1.69	**1.66**	1.46	1.43	1.05
0.0049	Non-avian theropods (purple)	**17.73**	**5.59**	**4.58**	**3.87**	**3.83**	**3.43**	**2.42**	**2.32**	**2.20**	**1.88**	1.61	1.58	1.39	1.36	-
0.0041	Psittaciformes	**13.03**	**4.11**	**3.36**	**2.84**	**2.82**	**2.52**	**1.78**	**1.70**	1.62	**1.38**	1.18	1.16	1.02	-	-
0.0034	Strigiformes	**12.76**	**4.03**	**3.29**	**2.78**	**2.76**	**2.47**	**1.74**	**1.67**	1.58	1.35	1.16	1.14	-	-	-
0.0034	Charadriiformes (most species)	**11.21**	3.54	**2.89**	**2.44**	**2.42**	**2.17**	**1.53**	**1.46**	1.39	1.19	1.02	-	-	-	-
0.0030	Anseriformes	**11.03**	3.48	**2.85**	2.41	2.38	2.13	1.51	1.44	1.37	1.17	-	-	-	-	-
0.0021	Paraves / early birds (grey)	**9.45**	2.98	**2.44**	**2.06**	**2.04**	**1.83**	1.29	1.23	1.17	-	-	-	-	-	-
0.0021	Birds of prey	**8.06**	2.54	**2.08**	1.76	1.74	1.56	1.10	1.05	-	-	-	-	-	-	-
0.0019	Picidae	**7.66**	2.41	**1.98**	1.67	**1.66**	1.48	1.05	-	-	-	-	-	-	-	-
0.0017	Aequornithia	**7.32**	2.31	**1.89**	1.60	**1.58**	**1.42**	-	-	-	-	-	-	-	-	-
0.0014	Ptilonorhynchidae	**5.17**	1.63	1.33	1.13	1.12	-	-	-	-	-	-	-	-	-	-
0.0014	“Intermediate” Neoaves (green)	**4.63**	1.46	1.19	1.01	-	-	-	-	-	-	-	-	-	-	-
0.0012	Coraciimorphae	**4.59**	1.45	1.18	-	-	-	-	-	-	-	-	-	-	-	-
0.0012	Passeriformes	**3.87**	1.22	-	-	-	-	-	-	-	-	-	-	-	-	-
0.0009	Apodiformes	3.17	-	-	-	-	-	-	-	-	-	-	-	-	-	-
0.0008	Charadriiformes (sandpipers/buttonquail)	-	-	-	-	-	-	-	-	-	-	-	-	-	-	-

Table 2. Comparison of rate of brain-body evolution between groups. Values represent ratios between group in first column and other groups. Values in bold represent statistically significant ($p<0.05$) differences between groups.

	Brain size			Body size		
Grade	Grade average	Δ Ancestral grade	Ratio	Grade average	Δ Ancestral grade	Ratio
Non-avian theropods (purple)	8.6	10.0	4.06	18.8	15.1	40.45
Apterygiformes: kiwi	9.2	8.6	1.82	14.5	15.1	0.55
Anseriformes: waterfowl	8.8	8.6	1.22	14.4	15.1	0.50
“Intermediate” Neoaves	7.9	8.6	0.50	12.5	15.1	0.07
Apodiformes: swifts & hummingbirds	6.1	7.9	0.17	9.8	12.5	0.07
Charadriiformes (part): sandpipers & buttonquail	7.0	7.9	0.41	11.4	12.5	0.33
Charadriiformes (part): other shorebirds	8.0	7.0	2.72	12.8	11.4	4.06
Aequornithia: waterbirds	8.8	7.9	2.46	13.6	12.5	3.00
Birds of prey: hawks, falcons, seiramas	9.3	7.9	4.06	14.4	12.5	6.69
Strigiformes: owls	8.6	9.3	0.50	12.5	14.4	0.15
Coraciimorphae: rollers & allies	7.3	9.3	0.14	11.2	14.4	0.04
Piciformes: woodpeckers	7.4	7.3	1.11	10.6	11.2	0.55
Psittaciformes: parrots	8.8	9.3	0.61	12.6	14.4	0.17
Passeriformes: passerines	6.9	9.3	0.09	10.4	14.4	0.02
Ptilonorhynchidae: bowerbirds	8.2	6.9	3.67	11.9	10.3	4.95
Corvidae: crows and ravens	8.4	6.9	4.48	12.0	10.3	5.47

Table 3. Comparisons of phylogenetic means across grades identified in this study versus their ancestral grade. ‘Grade average’ indicates the phylogenetic mean of brain and body size. ‘Δ ancestral grade’ indicates the shift in the phylogenetic mean between each grade and its ancestral grade. ‘Ratio’ indicates the ratio of the (unlogged) phylogenetic mean value of the listed grade relative to that of its ancestral grade.

STAR★METHODS

KEY RESOURCES TABLE

REAGENT or RESOURCE	SOURCE	IDENTIFIER
Deposited Data		
Endocast Volume and Body Mass Dataset	This paper	Data S1
Constraint topology for analyses with Jarvis tree	This paper	Data S2
Taxon reconciliation table	This paper	Data S3
Final tree using Jarvis constraint, used in downstream analyses	This paper	Data S4
Software and Algorithms		
R package 'bayou' V 2.1.1	https://github.com/uyedaj/bayou R package 'l1ou' V 1.40	N/A
R package 'l1ou' V 1.40	https://github.com/khabbazian/l1ou R package 'SURFACE' V 0.4-1	N/A
R package 'SURFACE' V 0.4-1	https://github.com/cran/surface R package 'evomap' V 2.0	N/A
R package 'evomap' V 2.0	https://github.com/JeroenSmaers/evomap	N/A
Mesquite V 3.03	http://mesquiteproject.org/	N/A
r8s	https://sourceforge.net/projects/r8s/	N/A

Contact for Reagent and Resource Sharing

Further information and requests for resources and reagents should be directed to and will be fulfilled by the Lead Contact, Daniel Ksepka (dksepka@brucemuseum.org).

Method Details

Brain-volume and Body-mass Data. We assembled a dataset of CT-rendered virtual endocasts to estimate brain volume, so as to facilitate sampling of rare and fossil taxa. Endocasts serve as a reliable proxy of the shape and volume of the brain in both birds and crownward non-avian theropods [47, 48]. We then combined this dataset with a recently published dataset based on lead-shot measurements of braincase volume [8]. Raw data and sources for taxa we sampled

534 directly are provided in the electronic file Dataset S1. We obtained body mass data from a
535 compendium [49] for most extant taxa. If the sex of a specimen was known, we used the average
536 body mass of the appropriate sex when available. Otherwise, the species average was taken. For
537 extinct birds where no body mass data were available from the literature, we applied body mass
538 regressions from femur circumference [50]. For non-avian theropods, we applied a bivariate
539 regression [51].
540
541 **Phylogeny and Divergence Dating.** As a phylogenetic backbone for the analysis of the
542 endocast dataset, we used the phylogeny of Jarvis et al [27] based on whole genomes from nearly
543 all 40+ avian orders. We generated a tree sampling ~6000 species using a pipeline approach [52].
544 This tree was then dated using a penalized likelihood approach in r8s v.1.7 [54, 55] with 21 fossil
545 calibrations (see Supplemental Information). We then pruned extant taxa not represented in our
546 dataset. Finally, extinct taxa for which no molecular data were available were grafted onto the
547 tree based on a recent phylogeny for non-avian theropod taxa [56] or recent
548 molecular/morphological phylogenies for each extinct bird species (see Data S1). Brain volume
549 and body mass were then input for all taxa in MESQUITE 3.04 [57].
550
551 **Characterizing Patterns of Allometric Integration.** We estimated differences in slope and
552 intercept of the brain-body relationship directly from the data using a Bayesian multi-regime
553 Ornstein Uhlenbeck (OU) modelling approach [58]. The OU model assumes that the evolution of
554 a continuous trait 'X' along a branch over time increment 't' is quantified as
555 $dX(t)=\alpha\left[\theta-X(t)\right]dt+\sigma dB(t)$ (59). Relative to the standard Brownian motion (BM) model (
556 $dX(t)=\sigma dB(t)$), the OU model adds parameters that estimate mean trait value (θ) and the rate at

557 which changes in mean values are observed (α). The inclusion of these additional parameters
558 allows an appropriate differentiation between changes in the mean (θ and α) and variance (σ) of
559 a trait over time and thus renders the OU model framework more appropriate than BM for
560 modelling changes in the direction of trait evolution. Here we used a bivariate implementation of
561 OU modeling that is explicitly geared towards estimating shifts in slope and intercept of
562 evolutionary allometries by using reversible-jump Markov chain Monte Carlo machinery (60;
563 'OUrjMCMC'). We implemented this approach by combining 10 parallel chains of 2 million
564 iterations each with a burn-in proportion of 0.3. We allowed only one shift per branch and the
565 total number of shifts was constrained by means of a conditional Poisson prior with a mean equal
566 to 2.5% of the total number of branches in the tree and a maximum number of shifts equal to 5%.
567 Starting points for MCMC chains were set by randomly drawing a number of shifts from the
568 prior distribution and assigning these shifts to branches randomly drawn from the phylogeny
569 with a probability proportional to the size of the clade descended from that branch. The MCMC
570 was initialized without any birth-death proposals for the first 10,000 generations to improve the
571 fit of the model. The output of this procedure generates an estimate of a best-fit allometric model
572 with posterior probabilities assigned to each shift in slope and/or intercept.
573 In part due to difficulties in parameter estimation intrinsic to OU modelling [61],
574 the bivariate OUrjMCMC output may include false positives and/or false negatives [60].
575 To identify false negatives, we ran a univariate OU model estimation procedure [21] on
576 the residuals of each grade in order to detect shifts in mean. If such shifts in mean were
577 detected, they were added as shifts in intercept to the allometric model (only the dinosaur
578 grade with the lowest intercept in the sample was detected using this procedure). To
579 identify false positives (including those that were added by the grade-specific univariate

analyses), the allometric model was translated to a least-squares framework and used in a confirmatory analysis using phylogenetic ANCOVA ('pANCOVA'; *21*). Even though pANCOVA uses a different evolutionary process than OU modelling (i.e. Brownian motion instead of Ornstein-Uhlenbeck), it is expected that grade membership as estimated by OU modelling is confirmed using least-squares analysis. Because Brownian motion assumes fewer statistical parameters, pANCOVA can be considered to be a conservative confirmatory test of the significance of grade membership as estimated by OU modeling.

Assessing the Strength of Allometric Integration. We compared rates of evolution among grades, applying a single intercept and single slope allometric model (one regression to fit entire sample), and between grades utilizing grade-specific allometric deviations. We compared rates after separating monophyletic clades for each grade (Table 2). We did not calculate rates for two clades (the moa *Emeus* + *Euryapteryx* and *Tyrannosaurus rex* + *Alioramus altai*) which include only two species as Brownian motion rates calculated based on so few data points cannot be considered valid. Lastly, we compared rates between Neoaves (treating corvids as a separate group) and earlier radiating clades (Table S2).

Assessing differential changes in brain and/or body size. To assess whether changes in the brain~body allometry were driven primarily by increase or decrease in either brain or body size, we calculated phylogenetic means for both brain size and body size for each of the allometric regimes identified by the best-fit allometric regime analysis described above using a procedure to calculate phylogenetic means [24], and implemented in the 'evomap' R package [25]. These

603 analyses identify differences in mean brain and/or body size between groups of species. Results
604 reveal the population averages in brain size and body size for the different allometric regimes.
605 Comparing shifts in mean average brain size and body size across regimes provides an indication
606 whether either shifts in brain size or body size primarily characterize shifts in allometric groups
607 (Table 3). For example, in the analysis of the endocast dataset the allometric grade comprising
608 corvids indicates a shift in (log) brain size of 1.5 and a shift in (log) body size of 1.7 relative to
609 its ancestral grade (the ratio of unlogged size changes relative to their ancestral grade is 4.48 for
610 brain size and 5.47 for body size, see Table 3). Considering that both the corvid grade and their
611 ancestral grade indicate negative allometry (with slopes of 0.66 and 0.65; Table 1), the general
612 expectation is that brain size changes at a slower pace relative to body size. Results for the shifts
613 in brain and body size in corvids, however, indicate that brain size changes more than body size
614 in this clade, even though there is also considerable change in body size. Given that changes in
615 brain size and body size are both positive, these results prompt the interpretation that crows and
616 ravens have increased both brain size and body size, but brain size more than body size given
617 allometric expectations.
618

SUPPLEMENTAL INFORMATION FOR:

Tempo and Pattern of Avian Brain Size Evolution

Daniel T. Ksepka, Amy M. Balanoff, N. Adam Smith, Gabriel S. Bever, Bhart-Anjan S. Bhullar, Estelle Bourdon, Edward L. Braun, J. Gordon Burleigh, Julia A. Clarke, Matthew W. Colbert, Jeremy R. Corfield, Federico J. Degrange, Vanesa L. De Pietri, Catherine M. Early, Daniel J. Field, Paul M. Gignac, Maria Eugenia Leone Gold, Rebecca T. Kimball, Soichiro Kawabe, Louis Lefebvre, Jesús Marugán-Lobón, Carrie S. Mongle, Ashley Morhardt, Mark A. Norell, Ryan C. Ridgely, Ryan S. Rothman, R. Paul Scofield, Claudia P. Tambussi, Christopher R. Torres, Marcel van Tuinen, Stig A. Walsh, Akinobu Watanabe, Lawrence M. Witmer, Alexandra K. Wright, Lindsay E. Zanno, Erich D. Jarvis, and Jeroen B. Smaers

Contents:

Additional details of phylogenetic methods. We used a ML constraint search strategy to generate the phylogeny used in downstream analyses. Specifically, we used the 48-taxon TENT (total evidence nucleotide) ML tree from the Jarvis et al. study [1] as a binary constraint tree (available as Data S2) in a ML analysis of an unpartitioned supermatrix [2] using a GTRCAT model in RAxML v. 8.2.10 [3]. In order to reconcile the taxa sampled in the constraint trees, the supermatrix, and our endocast dataset, we substituted closely related species in a few cases. These are listed in Dataset S3. Trees were dated using a penalized likelihood approach in r8s v.1.7 [4, 5] and 21 fossil calibrations (see below). This method was preferred here because a Bayesian divergence time estimation analysis is not computationally feasible for our large primary dataset. We applied a maximum constraint of 110 Ma for the age of Aves, which conservatively encompasses the age of the fossil ornithurine *Gansus yumenensis* but does not extend to the age of the Yixian Formation of China (125 Ma), which has yielded hundreds of stem birds but no crown birds and constrained the age of Neoaves to 66 Ma as no neoavian birds have been recovered from Cretaceous deposits. We selected the optimal smoothing parameter [10] based on a cross-validation analysis in which the age of crown Psittacopasserae was fixed to 60 Ma. Each fossil taxon was assigned a tip age based on the midpoint of the age range for the fossil specimen from which the endocast was generated. If a branch age was not available, we grafted the terminal branch to the midpoint of the internal branch from which it diverged. In cases where a zero length branch would result from grafting a fossil, 1 million years was added to the relevant branch.

Additional details of comparative methods. Our analyses identified an allometric model with four slopes and eleven intercepts as the best-fit model (Fig. 1A, Figs. S1-S12). This multi-grade model provides a significantly better fit to the data than a one grade model ($F_{15,2}$=29.56, P<0.001, AICΔ=343.53, AICω>0.99), and to a model that includes only differences in intercepts ($F_{15,12}$=52.11, P<0.001). Regression parameters of each of the seven grades are listed in Table S1. Each grade in this eleven-grade model is significantly different from its ancestral grade (Table S2). An alternative allometric model derived from a more conservative posterior probability cut-off (0.2 instead of 0.1) of the OUrjMCMC procedure did not identify separate grades for falcons, seriama, swifts and hummingbirds, buttonquail and sandpipers, and waterbirds. This alternative model, however, yields a significantly lower fit ($F_{15,11}$=11.21, P<0.001).

Mapping the identified scaling relationships across phylogeny, we identify independent evolutionary shifts away from the ancestral pattern of covariation of the brain-body scaling relationship in nine clades. Seven clades shift to a higher slope: Apterygiformes, Neoaves (excluding Phoenicopterimorphae and Columbimorphae), Apodiformes, a subset of Charadriiformes, Aequornithia, Coraciimorphae, and Psittacopasserae (Fig. 1). These clades exhibit a higher slope than other birds, with brain volume accordingly changing more rapidly relative to changes in body size. Two clades shift to a lower slope, conversely indicating slower change in brain size relative to body size: core Lari and Telluraves.

Because non-avian dinosaurs show a much larger range of body sizes and also exhibit more uncertainty in body size (since this must be estimated from limb bone proportions rather than measured directly), there is a possibility they may skew results near the base of the tree. We tested the impact of including fossils by comparing the

grades identified in the best-fit model in our complete tree and in a tree excluding fossils. The same eleven grades were identified in both analyses (Fig. S2D), demonstrating that the inclusion of non-avian dinosaurs does not drive the patterns identified in early-diverging birds.

Considering that previous work has suggested a shift in relative brain size along the phylogenetic interval between *Archaeopteryx* and the base of the crown bird radiation, we performed additional analyses to evaluate the fit of this scenario as well. We adjusted the best fit allometric model derived from our analyses to require a shift along the avian stem lineage and tested this model against our best-fit model ('adjusted best-fit' scenario in Fig. S2B). Results indicate that assuming a shift along the avian stem lineage yields a significantly worse fit than the alternative scenario ($AIC\Delta=19.51$, $AIC\omega<0.99$ in favor of the best-fit model).

Finally, we note that our methods allow non-monophyletic assemblages of taxa to occupy the same grade, which implies that some groups of birds may converge on the same regime independently. In order to control for the impact of clades sharing a grade but differing in rate, we treated each clade that shows a shift separately in the rate analysis.

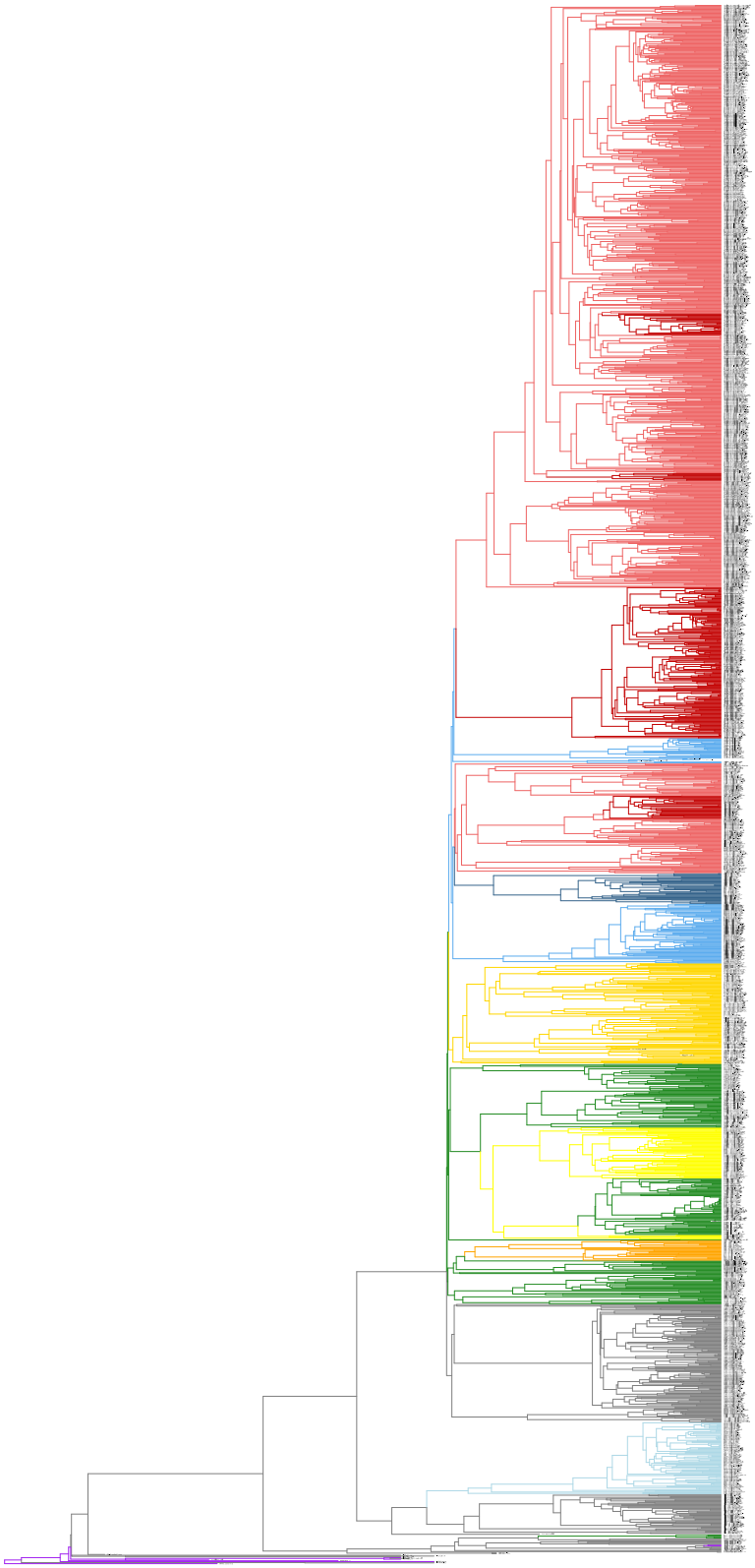

Figure S1. Complete phylogeny used in analyses. Colors correspond to the grades in Figure 1.

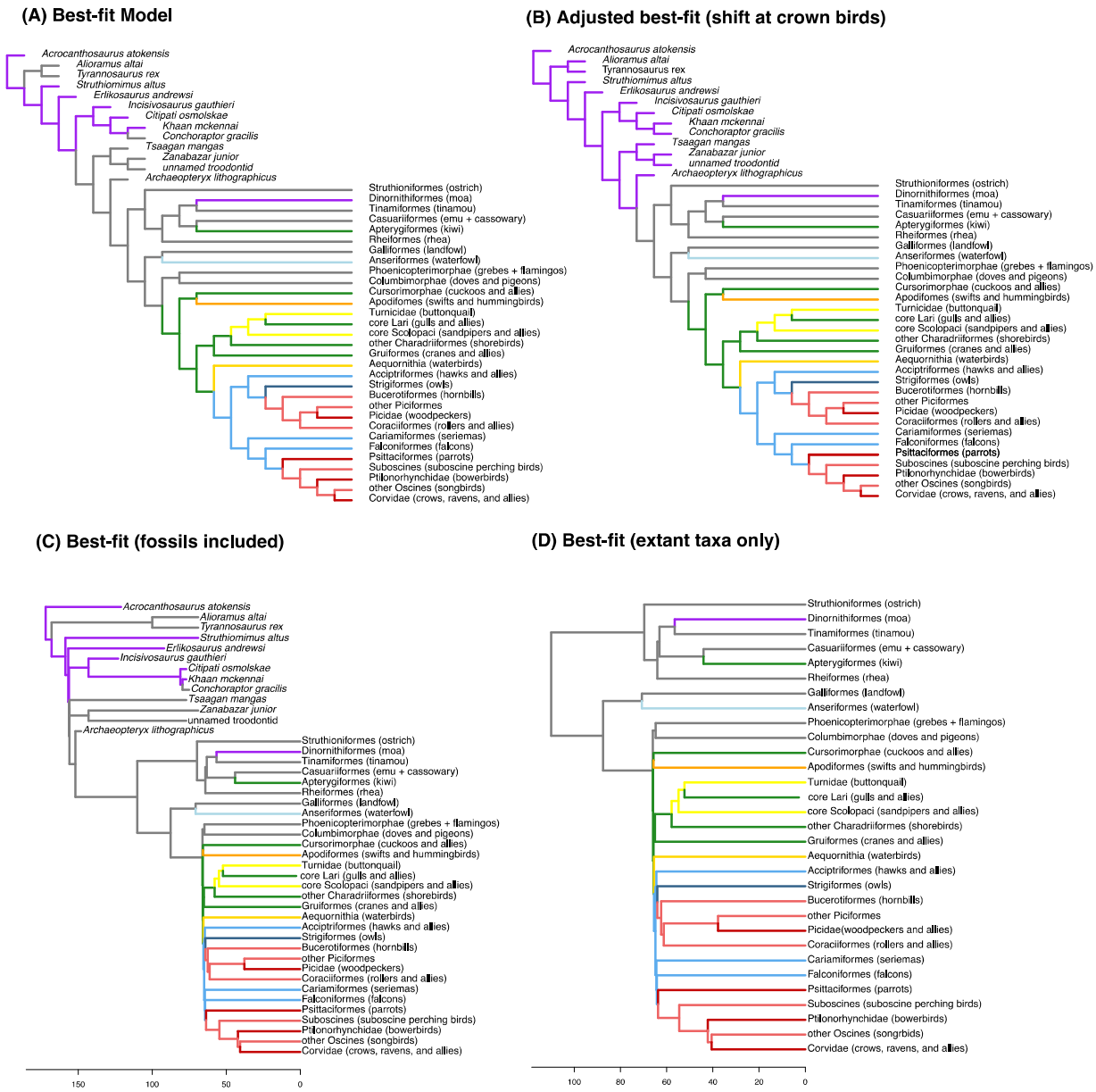

Figure. S2. (A+B) Comparison of the best-fit model identified in this study with an alternative model adjusted to accommodate a shift along the lineage immediately ancestral to crown birds. For visual clarity branch lengths were adjusted and thus do not represent time. (C+D) Exploration of the impact of including fossil taxa, comparing primary results (which include both

fossil and extant taxa) with analyses sampling only extant taxa. Branch lengths represent time. Colors correspond to the grades identified in Figure 1.

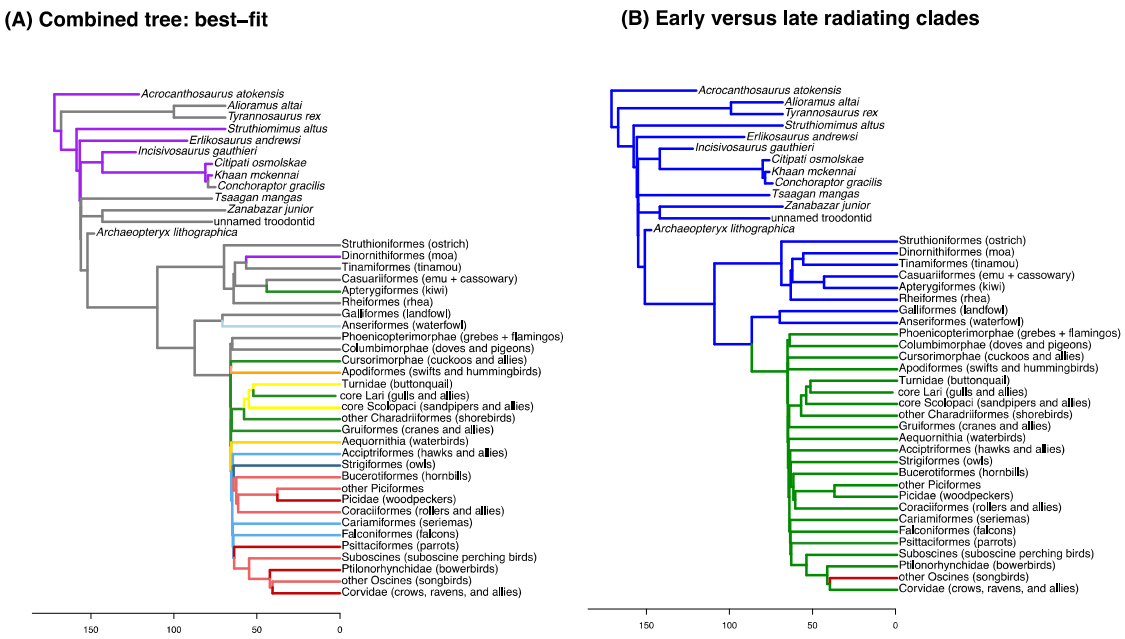

Figure S3. Overview of scenarios used in rate comparison tests. (A+B) The 'early versus late' scenario compares the earliest-branching crown bird clades (Palaeognathae and Galloanserae) against Neoaves (excluding parrots and corvids). Branch lengths represent time. Colors correspond to the grades identified in Figure 1.

	AIC Δ	AICw
DINO low	39.91	>0.99
Moa	20.18	>0.99
Kiwi	7.05	0.97
Waterfowl	83.17	>0.99
Green	7.67	0.98
Sandpipers	17.34	>0.99
Gulls Auks	7.77	0.98
Waterbirds	16.01	>0.99
Light blue	13.51	>0.99
Owls	3.34	0.84
Cavity birds	35.15	>0.99
Woodpeckers	19.37	>0.99
Parrots	57.62	>0.99
Passerines	100.57	>0.99
Bowerbirds	5.74	0.95
Corvids	13.12	>0.99

Table S1. pANCOVA Maximum Likelihood modeling analysis to test whether each grade contributes significantly to the overall fit of the model. In this analysis each identified monophyletic grade was removed from the analysis and its statistical fit (using AIC) was compared to the complete model. Results indicate the support for the complete model. In each instance, there is significant support for the complete model. This means that for each grade, there is significant statistical support for its inclusion.

	Fossil	Extant
Early v Late	1.88***	1.56***
Early v Late v Corvids	2.11***	1.75***

Table S2. Rate ratio comparisons and associated *P*-values among grades indicated in the trees of Figures S2 and S3. Rates of evolution were calculated on pGLS residuals, hereby measuring the strength of allometric integration. The rate ratio is a ratio of the rate observed in the earlier radiating group (Palaeognathae and Galloanserae; 'Early') relative to the rate observed in later radiating group (Neoaves; 'Late'). Significance testing was attained using permutation analysis. Considering the high rate in corvids, separate tests were included when considering corvids as a distinct group (i.e. excluding corvids from 'Late' and considering them separately). Fossil results are from trees including all taxa, extant results are from trees including extant taxa only. P-values indicated by asterisks: *p<0.05; **p<0.01; ***p<0.001.

Supplemental Information 1: Fossil calibrations used for dating the tree

Calibrated Node: Crown Casuariiformes (*Dromaius* – *Casuarius* split)

Fossil Specimen: *Emuarius gidju* QM F45460

Phylogenetic Justification: Worthy et al. [12] recovered *Emuarius* as more closely related to *Dromaius* than *Casuarius* in a phylogenetic analysis. Codings for *Emuarius* were based on multiple specimens, and key synapomorphies occur in the skull, tarsometatarsus and scapulocoracoid. A scapulocoracoid (QM F45460) is thus specified as the calibrating specimen.

Minimum Age Constraint: 24.5Ma

Maximum Age Constraint: 58.7Ma

Age Justification: The calibrating fossil is from Faunal Zone A at the Hiatus South Site of the Riversleigh locality in Queensland, Australia. Based on biocorrelation to the faunas from the Etadunna and Namba Formations in South Australia [13,14], a minimum age matching the top of Chron 7r is applied, with the numerical date selected from table 28.2 of [15]. The maximum is based on the age of the oldest putative palaeognaths, which include middle-late Paleocene lithornithids from North America and the ratite *Diogenornis*, from the early Eocene of Brazil. While the precise phylogenetic relationships of these taxa are debated, none are plausibly nested within crown Casuariiformes.

Calibrated Node: Stem Phasianidae (Phasianidae – Odontophoridae split)

Fossil Specimen: *Palaeortyx* cf. *gallica* PW 2005/5023a-LS

Phylogenetic Justification: Mayr et al. [16] described apomorphies including the well-developed processus intermetacarpalis that support placement of *Palaeortyx* cf. *gallica* within crown Galliformes, most likely as a stem group representative of Phasianidae. PW 2005/5023a-LS represents a nearly complete skeleton and thus is selected as the calibrating specimen.

Minimum Age Constraint: 24Ma

Maximum Age Constraint: 51.81Ma

Age Justification: The fossil is from a maar lake deposit at Enspel, near Bad Marienberg in Westerwald, Rheinland-Pfalz, Germany. These deposits are assigned to the MP28 biozone [17], the top of which is used for the hard minimum age. The maximum is based on the age of the Green River Formation from which multiple complete skeletons the stem galliform *Gallinuloides wyomingensis* have been collected. This maximum encompasses other strata that have yielded good material of stem galliforms but no convincing crown galliform material including the Messel Formation, Late Eocene horizons at Quercy, and the London Clay Formation. The maximum also encompasses the ages of taxa that may possibly represent crown galliforms but require additional study such as *Procrax* and *Schaubortyx.*

Calibrated Node: Crown Podicipediformes (MRCA of extant Podicipediformes]

Fossil Specimen: *Thiornis sociata* MNHN 1930–1

Phylogenetic Justification: Phylogenetic analysis by Ksepka et al. [18] places *Thiornis sociata* within a clade including *Poliocephalus* and *Tachybaptus,* which is in turn sister to *Dominicus dominicus*.

Minimum Age Constraint: 8.7 Ma

Maximum Age Constraint: 33.5 Ma

Age Justification: The fossil is from the Libros Gypsum of Teruel, Spain. The Libros Gypsum is considered Vallesian (Late Miocene) in age [19,20]. Because the Vallesian is a European mammal age defined by the appearance of mammal taxa (which may appear asynchronously at different localities), tying it to precise absolute dates remains difficult. Within Spain, the Vallesian is estimated to span 8.7–11.1Ma [21], the minimum end of which we use as a minimum age. The maximum is based on the oldest reported record of Mirandornithes, *Adelalopus hoogbutseliensis* from the early Oligocene of Belgium (MP21) [22].

Calibrated Node: Stem Mirandornithes (Mirandornithes – Charadriiformes split)

Fossil Specimen: *Juncitarsus merkeli* SMF A 295 (cast)

Phylogenetic Justification: Mayr [23] presented evidence for four synapomorphies linking *Juncitarsus* to Podicipediformes + Phoenicopteriformes, and also listed primitive characters which rule out placement of this taxon within crown Mirandornithes

Minimum Age Constraint: 46.6 Ma

Maximum Age Constraint: 61.6 Ma

Age Justification: The fossil is from the Messel Formation. A maximum age for the fossiliferous deposits of the Messel Formation is provided by a 47.8 ± 0.2 Ma 40Ar/39Ar age obtained from the basalt chimney below Lake Messel [24]. This date provides a maximum age for Lake Messel itself, but a minimum age for the fossil must take into account time elapsed between the cooling of the basalt and the deposition of the fossiliferous layers which occur higher in the section. Lacustrine sediments are estimated to have filled in the maar lake that formed above this basalt chimney over a span of approximately 1 Myr [25]. Accounting for sedimentation rate, the layers yielding avian fossils (including SMF-ME 1883a+b) are most

likely ~47 Ma in age [24,25]. When both the error range associated with the dating of the basalt (±0.2 Ma) and the estimate of time spanned between this date and deposition of the fossil (1 Ma) are incorporated, the hard minimum age for the fossil is 46.6 Ma. We use the upper age range estimate reported for the oldest aquatic neoavian, *Waimanu manneringi* as a maximum age.

Calibrated Node: Stem Steatornithidae (Steatornithidae – Nyctibiidae split)

Fossil Specimen: *Prefica nivea* USNM 336278

Phylogenetic Justification: Olson [26] discussed synapomorphies of *Prefica* and *Steatornis*, and a sister group relationship between the two was supported by the phylogenetic analysis of Mayr (2005).

Minimum Age Constraint: 51.81Ma

Maximum Age Constraint: 66.5Ma

Age Justification: The fossil is from Fossil Butte Member, Green River Formation, Wyoming, USA. These deposits are late early Eocene, and multicrystal analyses (sanidine) from a K-feldspar tuff (FQ-1) at the top of the middle unit of the Fossil Butte Member, from Fossil-Fowkes Basin (locality: N41º47'32.2" W110º42'39.6") have yielded an age of 51.97 ± 0.16Ma [27]. The latest Cretaceous is set as the soft maximum, corresponding to the age range of the oldest known neognathous bird *Vegavis iaii*. No members of Strisores are known from Cretaceous deposits, indicating it is unlikely the highly nested divergence between oilbirds and other Strisores had occurred before the Paleocene.

Calibrated Node: Crown Apodiformes (Apodidae/Hemiprocnidae – Trochilidae split)

Fossil Specimen: *Scaniacypselus wardi* NHMUKA5430

Phylogenetic Justification: Phylogenetic analyses have consistently placed *Scaniacypselus* as the sister taxon to extant Apodidae [28-30].

Minimum Age Constraint: 51Ma

Maximum Age Constraint: 66.5Ma

Age Justification: The fossil is from Bed R6 of the Røsnæs Clay Formation of Ølst, Denmark. Thiede et al. [31] assigned the upper calcareous beds of the Røsnæs Clay Formation, including R5 and R6 to nanoplankton biozones NP11 and NP12. Biostratigraphy supports correlation of the Røsnæs Clay Formation to the European mammal reference biozone MP8 [32], which suggests an age >50Ma [15]. A conservative minimum age of 51Ma is proposed, based specifically on the estimated age of the upper boundary of NP12, which is dated to 51Ma [15]. The latest Cretaceous is set as the maximum, corresponding to the age range of the oldest neognathous bird *Vegavis iaii*. No members of Strisores are known from Cretaceous deposits, indicating it is unlikely the highly nested divergence between swifts and hummingbirds had occurred before the Paleocene.

Calibrated Node: Crown Gruiformes (Ralloidea – Gruoidea split)

Fossil Specimen: *Pellornis mikkelseni* MGUH 29278

Phylogenetic Justification: Messelornithidae has been supported by synapomorphies as sister taxon to Rallidae+Heliornithidae [33] or Rallidae to the exclusion of Heliornithidae [34]. The more conservative placement (in terms of node depth) is used here.

Minimum Age Constraint: 53.9Ma

Maximum Age Constraint: 66.5Ma

Age Justification: The fossil is from the Fur Formation of Denmark. The minimum age is based on a 54.04+/-0.14Ma radiometric date reported for layer +19 of the Fur Formation [35]. The latest Cretaceous is set as the maximum, corresponding to the age range of the oldest neognathous bird *Vegavis iaii*. No reliable records of Gruiformes are known from Cretaceous deposits. This maximum incorporates the possibility that Paleocene taxa such as the poorly known *Messelornis russelli* or the enigmatic *Walbeckornis* belong to crown Gruiformes.

Calibrated Node: Crown Laridae

Fossil Specimen: *Laricola elegans* NMB s.g.18810

Phylogenetic Justification: De Pietri et al [36] recovered *Laricola* as either the sister to Laridae (=Laromorphae) or within Laridae (with *Anous* the sister taxon to all other Laridae). Smith [37] recommended *Laricola* as a crown Laromorphae calibration, however, the analysis upon which this was based was conducted before new cranial material was described. We conservatively place it as sister to Laromorphae, reflecting this uncertainty.

Minimum Age Constraint: 20.44Ma

Maximum Age Constraint: 47.8Ma

Age Justification: The fossil is from Saint-Gérand-le-Puy, France. Quarries at Saint-Gérand-le-Puy span the Oligocene and Miocene, but De Pietri et al [36] were unable to confirm or refute whether any of the historically collected *Laricola* material comes from the Oligocene age deposits. We thus conservatively use the upper bound of the Aquitanian for the hard minimum. The oldest reasonably complete fossil assignable to Charadriiformes is an unnamed Eocene (Lutetian) fossil SMF-ME 2458A+B [38]. The lower bound of the Lutetian is thus used as a maximum.

Calibrated Node: Stem Phaethontiformes

Fossil Specimen: *Lithoptila abdounensis* OCP.DEK/GE 1087

Phylogenetic Justification: Phylogenetic analyses by Bourdon et al. [39] and Smith [42] recover *Lithoptila abdounensis* as a stem representative of Phaethontiformes, and cranial characters preserved in OCP.DEK/GE 1087 support this placement. Although the position of Phaethontidae within Aves is controversial, there is no doubt regarding the placement of *Lithoptila*, which tracks Phaethontidae regardless of the arrangement of other taxa.

Minimum Age Constraint: 56Ma

Maximum Age Constraint: 72.1Ma

Age Justification: The fossil was collected from an unspecified quarry, assigned to Bed IIa of the Ouled Abdoun Basin, near Grand Daoui, Morocco, which in turn can be assigned to the Thanetian based on selachians identified in the matrix [41]. As both the precise numerical age of Bed IIa deposits and the precise horizon from which the fossil was collected remain uncertain, the lower age bound for the Thanetian is used as a hard minimum. More fragmentary records of probable Phaethontiformes are known from slightly older (Danian) deposits in New Zealand [40]. We conservatively rely on *Lithoptila*, but note that these records are encompassed between the minimum and maximum bounds. The maximum age extends to the base of the Maastrichtian to accommodate the possibility that some of the poorly represented marine birds from the Cretaceous-Paleogene of New Jersey may represent tropicbirds [41].

Calibrated Node: Stem Phalacrocoracidae (Phalacrocoracidae – Anhingidae split)

Fossil Specimen: *Oligocorax (=Borvocarbo) stoeffelensis* PW 2005/5022-LS

Phylogenetic Justification: Phylogenetic analysis by Smith [42] and Mayr [43] recover *Oligocorax stoeffelensis* as more closely related to *Phalacrocorax* than to *Anhinga*. PW 2005/5022-LS preserves a substantial portion of the skeleton, including synapomorphy-bearing elements.

Minimum Age Constraint: 24.82 Ma

Maximum Age Constraint: 51.81 Ma

Age Justification: The fossil is from a maar lake deposit at Enspel in Germany. These deposits are assigned to the MP28 biozone [43], the top of which is used for the hard minimum age. Comparable in age is the Late Oligeocene *Nambashag* from the Australian Etadunna and Namba Formations [44], which also represents a stem member of Phalacrocoracidae [43]. The maximum is based on the age of the Green River Formation, from which members of Aequornithes such as *Limnofregata* and *Vadaravis* have been recovered.

Calibrated Node: Crown Austrodyptornithes (Sphenisciformes-Procellariiformes split)

Fossil Specimen: *Waimanu maneringi* CM zfa35

Phylogenetic Justification: Phylogenetic analysis supports the placement of *Waimanu* along the stem penguin lineage [e.g. 45,46]. CM zfa35 is the only published specimen of *Waimanu manneringi.*

Minimum Age Constraint: 60.5Ma

Maximum Age Constraint: 72.1Ma

Age Justification: Biostratigraphic evidence, specifically the ranges of *Hornibrookina teuriensis* and *Chaismolithus bidens* indicate the minimum possible age of the type locality is 60.5 Ma [45,47,48]. The maximum is based on the lower bound of the Maastrichtian Stage.

923 Southern Hemisphere Maastrichtian marine vertebrate sites have yielded diving birds such as
924 *Polarornis* and hesperornithids, indicating preservation potential for marine diving birds, but no
925 penguin (or procellariiform) remains have been recovered at these sites.
926
927 **Calibrated Node:** Stem Fregatidae (Fregatidae – Suloidea split)
928 **Fossil Specimen:** *Limnofregata azygosternon* USNM 22753
929 **Phylogenetic Justification:** Phylogenetic analysis supports the placement of *Limnofregata* as
930 the sister taxon to extant *Fregata* [42], in agreement with longstanding interpretations of this
931 fossil taxon [26]. USNM 22753 is an articulated skeleton preserving most key synapomorphies
932 that place *Limnofregata azygosternon* on the frigatebird stem lineage.
933 **Minimum Age Constraint:** 51.57Ma
934 **Maximum Age Constraint:** 66.5Ma
935 **Age Justification:** The minimum date of 51.57Ma incorporates the error associated with an ^{40}Ar/
936 ^{39}Ar date of 51.66 ± 0.09Ma obtained from a potassium-feldspar (K-spar) tuff above the
937 fossiliferous horizon containing USNM 336484 [27]. A few fragmentary records of
938 *Limnofregata* are known from slightly older (~2Ma) deposits of the Wasatch Formation [49] and
939 Namejoy Formation [50]. We conservatively rely on the complete Fossil Butte skeleton, but note
940 that these records are encompassed between the minimum and maximum bounds. The latest
941 Cretaceous is set as the soft maximum, corresponding to the age range of the oldest known
942 crown bird *Vegavis*. No well-supported material from the core waterbird clade Aequornithes are
943 known from Cretaceous deposits, indicating it is unlikely the highly nested divergence between
944 Fregatidae and Suloidea had occurred before the Paleocene.
945

Calibrated Node: Crown Spheniscidae (MRCA extant Spheniscidae)

Fossil Specimen: *Spheniscus muizoni* MNHN PPI 147

Phylogenetic Justification: Synapomorphies were listed by Gölich [51] and this placement is supported by several subsequent phylogenetic analyses [e.g. 52]

Minimum Age Constraint: 9.2 Ma

Maximum Age Constraint: 27 Ma

Age Justification: In the original description [51] an age estimate of 11-13 Ma was provided for this fossil. However, subsequent work [53] shows this section to be younger in age. The maximum extends into the Late Oligocene, encompassing well-described fossil penguin faunas from the Late Oligocene-Early Miocene of New Zealand and South America which have yielded many articulated and associate skeletons of multiple species of stem lineage penguins but no reliable records of crown penguins.

Calibrated Node: Stem Threskiornithidae (Threskiornithidae – Pelecanidae/Ardeidae split)

Fossil Specimen: *Rhynchaeites* sp. MGUH 20288

Phylogenetic Justification: Multiple apomorphies support the placement of *Rhynchaeites* within the total clade Threskiornithidae [54]. Although the characteristic ibis-type bill is not preserved in MGUH 20288, derived characteristics of the hindlimb support assignment to *Rhynchaeites* as well as placement along the stem lineage of Threskiornithidae for this specimen [54].

Minimum Age Constraint: 53.9Ma

Maximum Age Constraint: 66.5Ma

Age Justification: The minimum age is based on a 54.04+/-0.14Ma radiometric date reported for layer +19 of the Fur Formation [35]. The latest Cretaceous is set as the soft maximum,

corresponding to the age range of the oldest neognathous bird *Vegavis.* No members of the core waterbird clade Aequornithes are known from Cretaceous deposits, indicating it is unlikely the highly nested divergence between ibises and other waterbirds occurred before the Paleocene.

Calibrated Node: Crown Piciformes (MRCA extant Piciformes)

Fossil Specimen: *Rupelramphastoides knopfi* SMF Av 500

Phylogenetic Justification: Mayr [55,56] provided evidence from synapomorphic features of the tarsometatarsus and ulna that clearly support placement of this fossil within total clade Pici. However, uncertainty remains over whether this taxon belongs within the crown Pici or is outside this clade. Conservatively, it is used as a calibration for the Pici-Galbulae split.

Minimum Age Constraint 31Ma

Maximum Age Constraint: 58.5Ma

Age Justification: The fossil is from Frauenweiler, Germany. The Frauenweiler locality is considered to be MP22 (32Ma) [57]. In order to set a hard minimum, the top of MP22 at 31Ma [48] was used. The maximum is based on the oldest described member of Afroaves, the Paleocene owl *Ogygoptynx wetmorei.*

Calibrated Node: Stem Coracii (Coracioidea – Meropidae split)

Fossil Specimen: *Primobucco mcgrewi* USNM 336484

Phylogenetic Justification: Phylogenetic analyses place *Primobucco mcgrewi* along the stem lineage leading to the clade Coracioidea (rollers and ground rollers) [58,59] This is consistent with the hypothesis originally proposed by Houde and Olson [60]

Minimum Age Constraint: 51.81Ma

Maximum Age Constraint: 66.5Ma

Age Justification: The fossil is from Fossil Butte Member, Green River Formation, Wyoming, USA. These deposits are late early Eocene, and multicrystal analyses (sanidine) from a K-feldspar tuff (FQ-1) at the top of the middle unit of the Fossil Butte Member, from Fossil-Fowkes Basin (locality: N41º47'32.2" W110º42'39.6") have yielded an age of 51.97 ± 0.16 Ma [27]. The latest Cretaceous is set as the maximum, corresponding to the age range of the oldest neognathous bird *Vegavis*. No members of the "landbird" clade Telluraves are known from Cretaceous deposits, indicating it is unlikely the highly nested Coracioidea – Meropidae divergence had occurred before the Paleocene.

Calibrated Node: Stem Todidae (Todidae – Momotidae/Alcedinidae split)

Fossil Specimen: *Palaeotodus itardiensis* SMF Av505

Phylogenetic Justification: Mayr and Knopf [61] identified derived characters of Todidae including the scapi clavicularum of the furcula being very thin, the proximal end of the humerus reaching far ventrally and being inflected so that almost the entire caput humeri is situated farther ventrally than the ventral margin of the shaft, a carpometacarpus with a large processus intermetacarpalis, a greatly elongated and slender tarsometatarsus measuring almost the length of the humerus, and the plantar surface of trochlea metatarsi III bearing a marked sulcus.

Minimum Age Constraint: 31Ma

Maximum Age Constraint: 55Ma

Age Justification: The fossil is from Frauenweiler south of Wiesloch (Baden-Württemberg, Germany), former clay pit of the Bott-Eder GmbH ("Grube Unterfeld"). The Frauenweiler locality was considered MP22 (32Ma) by Micklich and Hildebrandt [57]. The top of MP22 at

31Ma [15] was used to set a hard minimum. The oldest reported Coraciiformes [*sensu* 62] are from the early Eocene. Given this limit and the absence of Todidae in Lagerstätten such as the Green River, Messel, London Clay, and Fur Formations which otherwise preserve an abundance of small birds, a maximum of 55Ma is specified.

Calibrated Node: Crown Falconidae

Fossil Specimen: *Pediohierax ramenta* USNM 13898

Phylogenetic Justification: Phylogenetic analysis [63] supports placement of *Pediohierax ramenta* as a crown member of Falconidae. All remains of this taxon are isolated bones, and the apomorphies supporting placement as sister to *Falco* occur in the humerus and tarsometatarsus. Therefore, a tarsometatarsus is chosen as the calibrating specimen.

Minimum Age Constraint: 16Ma

Maximum Age Constraint: 57Ma

Age Justification: The fossil is from the Merychippus Quarry, Sand Canyon Member of the Sheep Creek Formation, Nebraska. The Sheep Creek Formation is assigned to the Hemmingfordian North American Land Mammal Age. Thus, the end of the Hemmingfordian is used as a minimum age for the calibration. There are many "raptorial" birds of uncertain affinities in the fossil record, which potentially represent Falconiformes, Accipitriformes, or some separate clade. The maximum extends back to the Eocene to include the taxon *Masillaraptor parvunguis.* This taxon is the oldest well-represented potential representative of Falconidae though its placement is far from resolved as it shares derived traits with many raptorial clades [64].

Calibrated Node: Crown Psittacopasserae

Fossil Specimen: *Pulchrapollia gracilis* NHMUK A6207

Phylogenetic Justification: Multiple phylogenetic analyses have recovered *Pulchrapollia gracilis* as a stem lineage parrot [65-67].

Minimum Age Constraint: 53.5 Ma

Maximum Age Constraint: 66.5 Ma

Age Justification: The fossil is from the Walton Member (Division A2) of the London Clay Formation at Walton-on-the-Naze, England. The Walton Member correlates to the upper part of Chron C24r, and the minimum age is based on the youngest estimate for the top of C24r (53.54+/-0.04 Ma) presented by Westerhold et al. [68] The latest Cretaceous is set as the maximum, corresponding to the age range of the oldest known crown bird *Vegavis*. No members of the "landbird" clade Telluraves (to which Psittacopasserae belong] are known from Cretaceous deposits, indicating it is extremely unlikely the highly nested parrot-songbird divergence had occurred before the Paleocene.

Calibrated Node: Crown Nestoridae

Fossil Specimen: *Nelepsittacus minimus* NMNZ S.52404

Phylogenetic Justification: Worthy et al. [69] reported several apomorphies that support a placement for *Nelepsittacus* closer to *Nestor* than to *Strigops.* A unique apomorphy, the foramen vasculare distale being bounded on its dorsal facies by a ridge extending proximal of it, creating a shallow groove extending proximal of the foramen, is observed in NMNZ S.52404.

Minimum Age Constraint: 15.9Ma

Maximum Age Constraint: none specified

Age Justification: The fossil is from Bed HH2b, Manuherikia River section, located 21.02–21.31 m above the base of the Bannockburn Formation. The Bannockburn Formation is considered to be Altonian in age. The numerical age is thus based on the upper boundary of the Altonian Stage. Given the sparse record of fossil parrots, we opt not to include a maximum constraint.

Calibrated Node: Crown Eupasseres

Fossil Specimen: Suboscines indet. SMNS 59466/1

Phylogenetic Justification: The presence of a distally-protruding fingerlike process at the cranial edge of metacarpal III is an apomorphic feature supporting assignment of SMNS 59466/1 to at least the suboscine stem lineage [70].

Minimum Age Constraint: 26Ma

Maximum Age Constraint: 55Ma

Age Justification: The fossil is from Ulm, Baden-Württemberg, Germany. Manegold [70] indicated an age of MP 28 based on a personal communication from Bötticher. Thus the lower age limit of MP 28 is used as a hard minimum age. The oldest reported Passeriformes are from the early Eocene Murgon site of Australia [71,72]. These fossils bear primitive characters that indicate they fall outside Eupasseres [73]. Furthermore, no crown Passeriformes of any type are found in Eocene deposits such as the Green River Formation and Messel Formation which otherwise preserve an abundance of small birds. Thus, the age of the Murgon fossils is used a soft maximum.

Supporting Information References

1. Jarvis, E.D. et al. (2014). Whole-genome analyses resolve early branches in the tree of life of modern birds. Science *346*, 1320-1331.
2. Burleigh, J.G., Kimball, R.T., and Braun, E.L. (2015). Building the avian tree of life using a large-scale sparse supermatrix. Molecular Phylogenetics and Evolution *84*, 53-63.
3. Stamatakis, A. (2014). RAxML version 8: a tool for phylogenetic analysis and post-analysis of large phylogenies. Bioinformatics *30*, 1312-1313.
4. Sanderson, M.J. (2003). r8s: inferring absolute rates of molecular evolution and divergence times in the absence of a molecular clock. Bioinformatics *19*, 301.
5. Prum, R.O. et al. (2015). A comprehensive phylogeny of birds (Aves) using targeted next-generation DNA sequencing. . Nature *526*, 569-573.
6. Smaers JB, Mongle CS (2018) evomap: R package for the evolutionary mapping of continuous traits: Github: https://github.com/JeroenSmaers/evomap dfa7dfd.
7. Sayol, F., Downing, P.A., Iwaniuk, A.N., Maspons, J., and Sol, D. (2018). Predictable evolution towards larger brains in birds colonizing oceanic islands. Nature Communications *9*, 2820.
8. Hackett, S.J., Kimball, R.T., Reddy, S., Bowie, R.C.K., Braun, E.L., Braun, M.J., Chojnowski, J.L., Cox, W.A., Han, K.-L., Harshman, J., et al. (2008). A phylogenomic study of birds reveals their evolutionary history. Science *320*, 1763-1768.
9. Ericson, P.G.P., Anderson, C.L., Britton, T., Elzanowski, A., Johansson, U.S., Källersjö, M., Ohlson, J.I., Parsons, T.J., Zuccon, D., and Mayr, G. (2006). Diversification of Neoaves: integration of molecular sequence data and fossils. Biology Letters *4*, 543-547.
10. Schliep KP (2010). phangorn: phylogenetic analysis in R. Bioinformatics *27*, 592-593.
11. Worthy TH, Hand SJ, Archer M (2014) Phylogenetic relationships of the Australian Oligo–Miocene ratite *Emuarius gidju* Casuariidae. *Integrative Zoology* 9: 148-166.
12. Woodburne, M.O., MacFadden, B.J., Case, J.A., Springer, M.S., Pledge, N.S., Power, J.D., Woodburne, J.M., and Springer, K.B. (1994). Land mammal biostratigraphy and magnetostratigraphy

of the Etadunna Formation (Late Oligocene) of South Australia. Journal of Vertebrate Paleontology*13*, 483–515.

13. Woodburne, M.O., Goin, F.J., Raigemborn, M.S., Heizler, M., Gelfo, J.N., and Oliveira, E.V. (2014). Revised timing of the South American early Paleogene land mammal ages. Journal of South American Earth Sciences *54*, 109-119.

14. Gradstein, F.M., Ogg, J.G., Schmitz, M., and Ogg, G. (2012). Geological Time Scale 2012, (Amsterdam: Elsevier Science and Technology).

15. Mayr, G., Poschmann, M., and Wuttke, M. (2006). A nearly complete skeleton of the fossil galliform bird *Palaeortyx* from the late Oligocene of Germany. . Acta Ornithologica *41*, 129–135.

16. Storch, G., Engesser, B., and Wuttke, M. (1996). Oldest fossil record of gliding in rodents. Nature *379*, 439–441.

17. Ksepka, D.T., Balanoff, A.M., Bell, M.A., and Houseman, M.D. (2013). Fossil grebes from the Truckee Formation (Miocene) of Nevada and a new phylogenetic analysis of Podicipediformes (Aves). Palaeontology *56*, 1149-1169.

18. Anadon, P. Cabrera, L. Julia, R. Roca, E. and Rosell, L. (1989) Lacustrine oil‐shale basins in Tertiary grabens from NE Spain (Western European rift system). Palaeogeography, Palaeoclimatology, Palaeoecology *70*, 7–28.

19. Ortí, F., Rosell, L., and Anadón, P. (2010). Diagenetic gypsum related to sulfur deposits in evaporites (Libros Gypsum, Miocene, NE Spain). Sedimentary Geology *228*, 304-318.

20. Garces, M., AgustÌ, J., Cabrera, L., and Pares, J.M. (1996). Magnetostratigraphy of the Vallesian (late Miocene) in the Valles-Penedes Basin (northeast Spain). Earth and Planetary Science Letters *142*, 381-396.

21. G. Mayr, R. Smith, Avian remains from the lowermost Oligocene of Hoogbutsel (Belgium). *Bulletin de l'Institut Royal des Sciences Naturelles de Belgique*, 72, 139–150 (2002).

22. G. Mayr, The Eocene *Juncitarsus* – its phylogenetic position and significance for the evolution and higher-level affinities of flamingos and grebes. *Comptes Rendus Palevol* 13, 9-18 (2014).

23. D. F. Mertz, F.-J. Harms, G. Gabriel, M. Felder, Arbeitstreffen in der Forschungsstation Grube Messel mit neuen Ergebnissen aus der Messel-Forschung. *Natur und Museum* 134, 289-290 (2004)

24. J. F. Franzen, The implications of the numerical dating of the Messel fossil deposit (Eocene, Germany) for mammalian biochronology. *Annales de Paléontologie* 91, 329-335 (2005).

25. Olson, S.L. (1977). A Lower Eocene frigatebird from the Green River Formation of Wyoming (Pelecaniformes, Fregatidae). Smithsonian Contributions to Paleontology *35*, 1-33.

26. M. E. Smith, K. R. Chamberlain, B. S. Singer, A. R. Carroll, Eocene clocks agree: Coeval 40Ar/39Ar, U-Pb, and astronomical ages from the Green River Formation. *Geology* 38, 527–530 (2010).

27. Mayr, G. (2005). A new cypselomorph bird from the middle Eocene of Germany and the early diversification of avian aerial insectivores. Condor *107*, 342-352.

28. Mayr, G. (2003). Phylogeny of early Tertiary swifts and hummingbirds (Aves: Apodiformes). Auk *120*, 145-151.

29. D. T. Ksepka, *et al*. Fossil evidence of wing shape in a stem relative of swifts and hummingbirds (Aves, Pan-Apodiformes). *Proceedings of the Royal Society B* 280, 20130580 (2013).

30. J. Thiede, O. B. Nielsen, K. Perch-Nielsen, Lithofacies, mineralogy and biostratigraphy of Eocene sediments in northern Denmark (Deep test Viborg 1). *Neues Jahrbuch für Geologie und Paläontologie, Abhandlungen,* 160*,149-172* (1980).

31. J. Mlíkovsky, Tertiary avian localities of Denmark. *Acta Universitatis Carolinae Geologica* 39, 559-562 (1996).

32. Mayr, G. (2004). Phylogenetic relationships of the early Tertiary Messel rails (Aves, Messelornithidae). Senckenbergiana Lethaea *84*, 317-322.

33. Bertelli, S., Chiappe, L.M., and Mayr, G. (2011). A new Messel rail from the Early Eocene Fur Formation of Denmark (Aves, Messelornithidae). . Journal of Systematic Palaeontology *9*, 551-562.

34. L. M. Chambers *et al.* Recalibration of the Palaeocene-Eocene boundary (P-E) using high precision U-Pb and Ar-Ar isotopic dating. *Geophysical Research Abstracts, EGS-AGU-EUG Joint Assembly,*

Nice, 6th-11th April 2003, 9681–9682 (2003).

35. V. L. De Pietri, L. Costeur, M. Güntert, G. Mayr, A revision of the Lari (Aves: Charadriiformes) from the early Miocene of Saint-Gérand-le-Puy (Allier, France). *Journal of Vertebrate Paleontology* 31, 812–828 (2011).

36. Smith, N.A. (2015). Sixteen vetted fossil calibrations for divergence dating of Charadriiformes (Aves, Neognathae). Palaeontologia Electronica *18.1.4FC*, 1-18.

37. G. Mayr, Charadriiform birds from the early Oligocene of Céreste (France) and the middle Eocene of Messel (Hessen, Germany). *Géobios* 33, 625-636 (2000).

38. E. Bourdon, Osteological evidence for sister group relationship between pseudo-toothed birds (Aves: Odontopterygiformes) and waterfowls (Anseriformes). *Naturwissenschaften* 92, 586-591 (2005).

39. G. Mayr, R. P. Scofield, New avian remains from the Paleocene of New Zealand: the first early Cenozoic Phaethontiformes (tropicbirds) from the Southern Hemisphere. *Journal of Vertebrate Paleontology* 36, e1031343 (2016).

40. E. Bourdon, C. Mourer-Chauviré, M. Amaghzaz, B. Bouya, New specimens of *Lithoptila abdounensis* (Aves, Prophaethontidae) from the Lower Paleogene of Morocco. *Journal of Vertebrate Paleontology* 28, 751-761 (2008).

41. N. D. Smith, Phylogenetic analysis of Pelecaniformes (Aves) based on osteological data: implications for waterbird phylogeny and fossil calibration studies. *PLoS ONE* 5, e13354 (2010).

42. G. Mayr, A new skeleton of the late Oligocene "Enspel cormorant"—from *Oligocorax* to *Borvocarbo*, and back again. *Palaeobiodiversity and Palaeoenvironments* 95:.87–101 (2015).

43. T. H. Worthy, Descriptions and phylogenetic relationships of a new genus and two new species of Oligo‐Miocene cormorants (Aves: Phalacrocoracidae) from Australia. *Zoological Journal of the Linnean Society* 163, 277-314 (2011).

44. Slack, K.E., Jones, C.M., Ando, T., Harrison, G.L., Fordyce, R.E., Arnason, U., and Penny, D. (2006). Early penguin fossils, plus mitochondrial genomes, calibrate avian evolution. Molecular Biology and Evolution 23, 1144-1155.

45. Ksepka, D.T., Bertelli, S., and Giannini, N.P. (2006). The phylogeny of the living and fossil Sphenisciformes (penguins). Cladistics *22*, 412-441.

46. R. A. Cooper, *The New Zealand Geological Timescale*. (Institute of Geological and Nuclear Sciences, 2004).

47. J. G. Ogg, G. Ogg, F. M. Gradstein, *The Concise Geologic Time Scale*. (Cambridge University Press, 2008).

48. Stidham, T.A. (2015). A new species of *Limnofregata* (Pelecaniformes: Fregatidae) from the Early Eocene Wasatch Formation of Wyoming: implications for palaeoecology and palaeobiology. Palaeontology *58*, 239-249.

49. G. Mayr, The world's smallest owl, the earliest unambiguous charadriiform bird, and other avian remains from the early Eocene Nanjemoy Formation of Virginia (USA). *PalZ 90*, 747–763 (2016).

50. U. B. Göhlich, The oldest fossil record of the extant penguin genus *Spheniscus* - a new species from the Miocene of Peru. *Acta Paleontologica Polonica* 52, 285-298 (2007).

51. Ksepka, D.T., and Clarke, J.A. (2010). The basal penguin (Aves: Sphenisciformes) *Perudyptes devriesi* and a phylogenetic evaluation of the penguin fossil record. Bulletin of the American Museum of Natural History *337*, 1-77.

52. L. Brand, *et al*.. A high resolution stratigraphic framework for the remarkable fossil cetacean assemblage of the Miocene/Pliocene Pisco Formation, Peru. *Journal of South American Earth Sciences* 31, 414-425 (2011).

53. Mayr, G., and Bertelli, S. (2011). A record of *Rhynchaeites* (Aves, Threskiornithidae) from the early Eocene Fur Formation of Denmark, and the affinities of the alleged parrot *Mopsitta*. Palaeobiodiversity and Palaeoenvironments *91*, 229-236.

54. Mayr, G. (2005). A tiny barbet-like bird from the lower Oligocene of Germany: the smallest species and earliest substantial fossil record of the pici (woodpeckers and allies). The Auk *122*, 1055-1063.

55. Mayr, G. (2006). First fossil skull of a Paleogene representative of the Pici (woodpeckers and allies) and its evolutionary implications. Ibis *148*, 824-827.

56. N. Micklich, L. Hildebrandt, The Frauenweiler clay pit (‘‘Grube Unterfeld’’). . *Kaupia: Darmstädter Beiträge zur Naturkunde* 14, 113–118 (2005).

57. Mayr, G., Mourer-Cliauviré, C., and Weidig, I. (2004). Osteology and systematic position of the Eocene Primobucconidae (Aves, Coraciiformes *sensu stricto*), with first records from Europe. Journal of Systematic Palaeontology *2*, 1-12.

58. Clarke, J.A., Ksepka, D.T., Smith, N.A., and Norell, M.A. (2009). Combined phylogenetic analysis of a new North American fossil species confirms widespread Eocene distribution for stem rollers (Aves, Coracii). Zoological Journal of the Linnean Society *157*, 586-611.

59. 1. Houde, P., and Olson, S. (1989). Small arboreal non-passerine birds from the early Tertiary of western North America. In Acta XIX Congressus Internationalis Ornithologici, H. Ouellet, ed. (Ottawa: University of Ottawa Press), pp. 2030–2036.

60. Mayr, G., and Knopf, C.W. (2007). A tody (Alcediniformes: Todidae) from the early Oligocene of Germany. The Auk *124*, 1294-1304.

61. Yuri, T., Kimball, R.T., Harshman, J., Bowie, R.C.K., Braun, M.J., Chojnowski, J.L., Han, K.-L., Hackett, S.J., Huddleston, C.J., Moore, W.S., et al. (2013). Parsimony and model-based analyses of indels in avian nuclear genes reveal congruent and incongruent phylogenetic signals. Biology *2*, 419-444.

62. Li, Z., Zhou, Z., Deng, T., Li, Q., and Clarke, J.A. (2014). A falconid from the Late Miocene of northwestern China yields further evidence of transition in Late Neogene steppe communities. Auk *131*, 335-350.

63. Mayr, G. (2009)/ A well-preserved skull of the “falconiform” bird *Masillaraptor* from the middle Eocene of Messel (Germany). Palaeodiversity *2*, 315-320.

64. Dyke, G.J., and Cooper, J.H. (2000). A new psittaciform bird from the London Clay (Lower Eocene) of England. Palaeontology *43*, 271-285.

65. G. Mayr, The postcranial osteology and phylogenetic position of the Middle Eocene *Messelastur gratulator* Peters, 1994; a morphological link between owls (Strigiformes) and falconiform birds?

Journal of Vertebrate Paleontology 25, 635-645 (2005).

66. Ksepka, D.T., Clarke, J.A., and Grande, L. (2011). Stem parrots (Aves, Halcyornithidae) from the Green River Formation and a combined phylogeny of Pan-Psittaciformes. Journal of Paleontology *85*, 835-854.

67. Westerhold, T., Röhl, U., Laskar, J., Raffi, I., Bowles, J., Lourens, L.J., and Zachos, J.C. (2007). On the duration of magnetochrons C24r and C25n and the timing of early Eocene global warming events: Implications from the Ocean Drilling Program Leg 208 Walvis Ridge depth transect. Paleoceanography *22*, PA2201.

68. Worthy, T.H., Tennyson, A.J.D., and Scofield, R.P. (2011). An Early Miocene diversity of parrots (Aves, Strigopidae, Nestorinae) from New Zealand. Journal of Vertebrate Paleontology *31*, 1102-1116.

69. Manegold, A. (2008). Passerine diversity in the late Oligocene of Germany: Earliest evidence for the sympatric coexistence of Suboscines and Oscines. Ibis *150*.

70. Boles, W.E. (1995). The world's earliest songbird (Aves: Passeriformes). Nature *374*, 21-22.

71. Boles, W.E. (1997). Fossil songbirds (Passeriformes) from the early Eocene of Australia. Emu *97*, 43-50.

72. Mayr, G. (2013). The age of the crown group of passerine birds and its evolutionary significance – molecular calibrations versus the fossil record. Systematics and Biodiversity *11*, 7–13.